 CMES, vol.731, no.1, pp.1-12, 2009

Derivation of Anti-Plane Dynamic Green's Function for Several Circular Inclusions with Imperfect Interfaces

Jeng-Tzong Chen[1] **nad Jia-Nan Ke**

Abstract: A null-field integral equation is employed to derive the two-dimensional antiplane dynamic Green's functions for a circular inclusion with an imperfect interface. We employ the linear spring model with vanishing thickness to characterize the imperfect interface. Analytical expressions of displacement and stress fields due to time-harmonic antiplane line forces located either in the unbounded matrix or in the circular inclusion are presented. To fully capture the circular geometries, degenerate- kernel expressions of fundamental solutions in the polar coordinate and Fourier series for boundary densities are adopted. Good agreement is made after comparing with the analytical solution derived by Wang and Sudak's results. Parameter study of wave number and interface constant is done. In this paper, we employ the null-field BIE to derive the analytical Green's function instead of choosing the Trefftz bases by using the Wang and Sudak's approach. Special cases of cavity and ideal bonding as well as static solutions are also examined. Besides, two-inclusions case in the matrix with a concentrated force problem is also solved.

Keyword: Time-harmonic Green's function, inclusion, imperfect interface, null-field integral equation, degenerate kernel, Fourier series.

1 Introduction

Analytical as well as numerical Green's functions have received many BEM researchers' attention [Ang (1987); Ang and Telles (2004); Hwu and Yen (1991)]. Boundary element method (BEM) was employed to solve time-harmonic Green's function [Kitahara (1985); Denda, Wang and Yong (2003); Denda, Araki and Yong (2004)]. Also, dynamic Eshelby problems [Mikata and Nemat-Nasser (1990); Cheng and Batra (1999); Michelitsch, Levin and Gao (2002)], piezoelectricity problems [Wang and Zhong (2003); Chen and Wu (2006); Yang and Tewary (2006); Wu and Chen (2007)] and scattering problems in elastodynamics [Willis (1980a, b); Talbot and Willis (1983)] were solved. Although a lot of papers on homogeneous case were published, only a few of the time-harmonic dynamic Green's functions of a circular cylindrical inclusion can be found [Mura (1988); Mura, Shodja and Hirose (1996)]. Recently, Wang and Sudak [Wang and Sudak (2007)] derived an analytical solution for antiplane time-harmonic Green's functions of a circular inhomogeneity with an imperfect interface [Ang and Fan (2004)]. The interface between the inclusion and the matrix is modeled to the linear springs with vanishing thickness. Interface boundary conditions are tractions equilibrium but the displacements across the interface are discontinuous. In addition, the stress response is proportional to the linear springs interface with vanishing thickness. The key concept of Wang and Sudak's method is that they introduced the Trefftz bases for the solution representation of inclusion and matrix, respectively. However, the completeness of Trefftz bases needs special case. Our main concern is to revisit the problem solved by Wang and Sudak and derive the analytical solution in an alternative way by using the null-field integral equation. Based on the null-field integral formulation, the analytical solution will be derived in a more systematic and straightforward way. Besides, special cases of cavity and ideal bonding as well as static solutions will be examined.

[1] Department of Harbor and River Engineering, National Taiwan Ocean University, Keelung, Taiwan

2 Derivation of anti-plane dynamic Green's function for Helmholtz problems with imperfect circular boundaries

2.1 Problem statement and null-field integral formulation

For a two-dimensional problem with an imperfect interface, we consider a unbounded matrix containing a circular inclusion of radius a with its centre at the origin. A time-harmonic antiplane line force ofstrength $pe^{-i\omega t}$ is located at $(e,0)$ on the x axis either in the inclusion $(0<e<a)$ or in the matrix $(a<e)$ as shown in Figs. 1(a) and 1(b). The μ_M and μ_I represent the shear moduli of matrix and inclusion, respectively. The antiplane displacement field subject to the concentrated load in the matrix is shown below

$$(\nabla^2+k_I^2)G(x,\xi)=-\frac{p}{\mu_I}\delta(x-\xi), \quad x\in D_I \quad \text{if } e<a \tag{1}$$

For the infinite matrix with a single inclusion subject to a concentrated load, we have

$$(\nabla^2+k_M^2)G(x,\xi)=-\frac{p}{\mu_M}\delta(x-\xi), \quad x\in D_M \quad \text{if } e>a \tag{2}$$

where ∇^2 is the Laplacian operator, k_I and k_M are the wave numbers for the inclusion and matrix, $\delta(x-\xi)$ denotes the Dirac-delta function, D_I and D_M are domains of the inclusion and matrix, respectively. The time factor $e^{-i\omega t}$ has been omitted due to the frequency-domain approach after employing the separable property. For a linear elastic body, the stress components are

$$\sigma_{zr}^I=\mu_I\frac{\partial u_I}{\partial r},\ \sigma_{z\theta}^I=\mu_I\frac{\partial u_I}{r\partial\theta}, \quad x\in D_I \tag{3}$$

$$\sigma_{zr}^M=\mu_M\frac{\partial u_M}{\partial r},\ \sigma_{z\theta}^M=\mu_M\frac{\partial u_M}{r\partial\theta}, \quad x\in D_M \tag{4}$$

Moreover, we presume that the circular boundary interface is imperfect and homogeneous in the angular direction [Ang, Choo and Fan (2004)]. The interface boundary conditions are given by [Hashin (1991); Ru and Schiavone (1997); Wang and Meguid (1999)].

$$\sigma_{zr}^I=\sigma_{zr}^M=\beta(u_M-u_I), \quad \text{on the interface } r=a \tag{5}$$

where the non-negative constant β is the parameter of imperfect interface. The circular inclusion is perfectly bonded to the matrix if β approaches infinity. On the other hand, the circular inclusion is fully debonded from the matrix if β approaches zero. In order to employ the Green's third identity as follows

$$\iint_D \left[u(x)\nabla^2 v(x)-v(x)\nabla^2 u(x)\right]dD(x) = \int_B \left[u(x)\frac{\partial v(x)}{\partial n}-v(x)\frac{\partial u(x)}{\partial n}\right]dB(x) \tag{6}$$

we need two systems, $u(x)$ and $v(x)$. We choose $u(x)$ as $G(x,\xi)$ and set $v(x)$ as the fundamental solution $U(x,s)$ such that

$$\nabla^2 U(x,s)=2\pi\delta(x-s) \tag{7}$$

Then, we can obtain the fundamental solution as follows

$$U(s,x)=\frac{-i\pi H_0^{(1)}(kr)}{2} \tag{8}$$

where $H_0^{(1)}(kr)$ is the zeroth Hankel function of the first kind and $r\equiv|s-x|$. In the present method, we adopt the mathematical tools, degenerate kernels, for the purpose of analytical study. The combination of degenerate kernels and Fourier series plays the major role in handling problems with circular boundaries. Based on the separable property, the kernel function $U(s,x)$ and $T(s,x)$ can be expanded into separable form by dividing the source point $s=(R,\theta)$ and field point $x=(\rho,\phi)$ in the polar coordinate [Chen, Liu and Hong (2003)]. After exchanging with the variables x and s, we have

$$2\pi G(x,\xi)=\int_B T(s,x)G(s,\xi)dB(s) - \int_B U(s,x)\frac{\partial G(s,\xi)}{\partial n_s}dB(s)+U(\xi,x), \quad x\in D \tag{9}$$

where $T(s,x)$ is defined by

$$T(s,x) \equiv \frac{\partial U(s,x)}{\partial n_s} \tag{10}$$

where n_s denotes the outward normal vector at the source point s. To solve the unknown boundary densities $G(s,\xi)$ and $\partial G/\partial n_s(s,\xi)$, the field point x is located outside the domain to yield the null-field integral equation as shown below:

$$\begin{aligned} 0 = & \int_B T(s,x)G(s,\xi)dB(s) \\ & - \int_B U(s,x)\frac{\partial G(s,\xi)}{\partial n_s}dB(s) + U(\xi,x), \quad x \in D^c \end{aligned} \tag{11}$$

where D^c is the complementary domain. By using the degenerate kernels, the BIE for the "boundary point" can be easily derived through either the null-field integral equation in Eq. (11) or the BIE for the domain point of Eq. (9) by exactly collocating x on B [Chen, Shen and Chen (2006)].

2.2 Expansion of kernel function and boundary density

Based on the separable property, the kernel function $U(s,x)$ can be expanded into series form by separating the field point $x(\rho,\phi)$ and source point $s(R,\theta)$ in the polar coordinate:

$$U(s,x) = \begin{cases} U^i(s,x) = \frac{-\pi i}{2}\sum\limits_{m=0}^{\infty}\varepsilon_m J_m(k\rho)H_m^{(1)}(kR) \\ \quad \cos(m(\theta-\phi)),\ R \geq \rho \\ U^e(s,x) = \frac{-\pi i}{2}\sum\limits_{m=0}^{\infty}\varepsilon_m H_m^{(1)}(k\rho)J_m(kR) \\ \quad \cos(m(\theta-\phi)),\ \rho > R \end{cases} \tag{12}$$

where the superscripts "i" and "e" denote the interior and exterior cases for the expressions of kernel, respectively, and ε_m is the Neumann factor

$$\varepsilon_m = \begin{cases} 1, & m = 0 \\ 2, & m = 1,2,\ldots\infty \end{cases} \tag{13}$$

It is noted that the larger argument is contained in the complex Hankel function to ensure the series convergence and log singularity. According to the definition of $T(s,x)$ in Eq. (10), we have

$$T(s,x) = \begin{cases} T^i(s,x) = \frac{-\pi ki}{2}\sum\limits_{m=0}^{\infty}\varepsilon_m J_m(k\rho)H_m'^{(1)}(kR) \\ \quad \cos(m(\theta-\phi)),\ R > \rho \\ T^e(s,x) = \frac{-\pi ki}{2}\sum\limits_{m=0}^{\infty}\varepsilon_m H_m^{(1)}(k\rho)J_m'(kR) \\ \quad \cos(m(\theta-\phi)),\ \rho > R \end{cases} \tag{14}$$

The unknown boundary densities can be represented by using the Fouries series as shown below:

$$G(s,\xi) = a_0 + \sum_{n=1}^{\infty}(a_n\cos n\theta + b_n\sin n\theta),\ \ s \in B \tag{15}$$

$$\frac{\partial G(s_k,\xi)}{\partial n_s} = p_0 + \sum_{n=1}^{\infty}(p_n\cos n\theta + q_n\sin n\theta) \tag{16}$$

where a_0, a_n, b_n, p_0, p_n and q_n are the Fourier coefficients. In the real computation, the integrations can be easily calculated by employing the orthogonal property of Fourier series, and only the finite M terms are used in the summation.

2.3 Series representation for the Green's function of an inclusion case

For the problems with inclusion, we can decompose into subsystems of matrix and inclusion after taking the free body on the interface as shown in Fig. 1(c). By collocating x on $(a-,\phi)$ and $(a+,\phi)$ for the matrix and inclusion, respectively,

the null-field equations yield

$$
\begin{aligned}
0 = & -a_0^e k_M \pi^2 a J_0(k_M a)\left[Y_0'(k_M a) - iJ_0'(k_M a)\right] \\
& - \sum_{m=1}^{\infty} \left(a_m^e \cos(m\phi) + b_m^e \sin(m\phi)\right) k_M \pi^2 a J_m(k_M a) \\
& \left[Y_m'(k_M a) - iJ_m'(k_M a)\right] \\
& - p_0^e \pi^2 a J_0(k_M a)\left[Y_0(k_M a) - iJ_0(k_M a)\right] \\
& - \sum_{m=1}^{\infty} \left(p_m^e \cos(m\phi) + q_m^e \sin(m\phi)\right) \pi^2 a J_m(k_M a) \\
& \left[Y_m(k_M a) - iJ_m(k_M a)\right] \\
& - \frac{p}{\mu_M}\Big\{\frac{\pi}{2} J_0(k_M a)[Y_0(k_M e) - iJ_0(k_M e)] \\
& + \sum_{m=1}^{\infty} \pi J_m(k_M a)[Y_m(k_M e) - iJ_m(k_M e)]\cos(m\phi)\Big\} \\
& \qquad\qquad x \to (a-,\phi) \quad (17)
\end{aligned}
$$

$$
\begin{aligned}
0 = & \, a_0^i k_I \pi^2 a J_0'(k_I a)\left[Y_0(k_I a) - iJ_0(k_I a)\right] \\
& + \sum_{m=1}^{\infty} \left(a_m^i \cos(m\phi) + b_m^i \sin(m\phi)\right) k_I \pi^2 a J_m'(k_I a) \\
& \left[Y_m(k_I a) - iJ_m(k_I a)\right] \\
& - p_0^i \pi^2 a J_0(k_I a)\left[Y_0(k_I a) - iJ_0(k_I a)\right] \\
& - \sum_{m=1}^{\infty} \left(p_m^i \cos(m\phi) + q_m^i \sin(m\phi)\right) \pi^2 a J_m(k_I a) \\
& \left[Y_m(k_I a) - iJ_m(k_I a)\right] \\
& \qquad\qquad x \to (a+,\phi) \quad (18)
\end{aligned}
$$

Interface conditions of Eq. (5) can be rewritten as

$$t^I = \frac{\beta}{\mu_I}(u^M - u^I), \quad \text{on the interface} \quad (19)$$

$$-\mu_M t^M = \mu_I t^I, \quad \text{on the interface} \quad (20)$$

By assembling the matrices in Eqs. (17), (18), (19) and (20), we have

$$
\begin{bmatrix} T_{11}^M & -U_{11}^M & 0 & 0 \\ 0 & 0 & T_{11}^I & -U_{11}^I \\ 0 & \mu_M & 0 & \mu_I \\ \beta & \mu_M & -\beta & 0 \end{bmatrix}
\begin{bmatrix} u_1^M \\ t_1^M \\ u_1^I \\ t_1^I \end{bmatrix}
= \begin{bmatrix} \frac{p}{\mu_M} U(\xi, x) \\ 0 \\ 0 \\ 0 \end{bmatrix} \quad (21)
$$

After rearranging Eq. (22), we have

$$
\begin{bmatrix} T_{11}^M & -U_{11}^M \\ T_{11}^I & \frac{\mu_M}{\beta} T_{11}^I + \frac{\mu_M}{\mu_I} U_{11}^I \end{bmatrix}
\begin{bmatrix} u_1^M \\ t_1^M \end{bmatrix}
= \begin{bmatrix} \frac{p}{\mu_M} U(\xi, x) \\ 0 \end{bmatrix} \quad (22)
$$

The unknown coefficients in the algebraic system can be determined as shown below:

$$
\begin{aligned}
a_0^e = & \\
& - p[J_0(k_M e) + iY_0(k_M e)][\beta J_0(k_I a) + k_I \mu_I J_0'(k_I a)] \\
& /2\pi a\Big\{k_I \mu_I J_0'(k_I a)[-\beta[J_0(k_M a) + iY_0(k_M a)] \\
& + k_M \mu_M [J_0'(k_M a) + iY_0'(k_M a)]] + \beta k_M \mu_M J_0(k_I a) \\
& \qquad [J_0'(k_M a) + iY_0'(k_M a)]\Big\} \quad (23)
\end{aligned}
$$

$$
\begin{aligned}
& p_0^e = p\beta k_I \mu_I [J_0(k_M e) + iY_0(k_M e)] J_0'(k_I a) \\
& /2\pi a \mu_M \Big\{k_I \mu_I J_0'(k_I a)[-\beta[J_0(k_M a) + iY_0(k_M a)] \\
& + k_M \mu_M [J_0'(k_M a) + iY_0'(k_M a)]] + \beta k_M \mu_M J_0(k_I a) \\
& \qquad [J_0'(k_M a) + iY_0'(k_M a)]\Big\} \quad (24)
\end{aligned}
$$

$$
\begin{aligned}
a_m^e = & \\
& - p[J_m(k_M e) + iY_m(k_M e)][\beta J_m(k_I a) + k_I \mu_I J_m'(k_I a)] \\
& /\pi a\Big\{k_I \mu_I J_m'(k_I a)[-\beta[J_m(k_M a) + iY_m(k_M a)] \\
& + k_M \mu_M [J_m'(k_M a) + iY_m'(k_M a)]] + \beta k_M \mu_M J_m(k_I a) \\
& \qquad [J_m'(k_M a) + iY_m'(k_M a)]\Big\} \quad (25)
\end{aligned}
$$

$$
\begin{aligned}
& p_m^e = p\beta k_I \mu_I [J_m(k_M e) + iY_m(k_M e)] J_m'(k_I a) \\
& /\pi a \mu_M \Big\{k_I \mu_I J_m'(k_I a)[-\beta[J_m(k_M a) + iY_m(k_M a)] \\
& + k_M \mu_M [J_m'(k_M a) + iY_m'(k_M a)]] + \beta k_M \mu_M J_m(k_I a) \\
& \qquad [J_m'(k_M a) + iY_m'(k_M a)]\Big\} \quad (26)
\end{aligned}
$$

where a_0^e, p_0^e, a_m^e and p_m^e, $m = 1, 2, 3, \ldots$ are the Fourier coefficients of boundary densities for the matrix. According to interface boundary condition of Eqs. (19) and (20), we obtain the Fourier coefficient of the inclusion as shown below:

$$
\begin{bmatrix} a_0^i \\ p_0^i \end{bmatrix}
= \begin{bmatrix} \frac{\mu_M}{\beta} p_0^e + a_0^e \\ 0 \end{bmatrix} \quad (27)
$$

$$\begin{bmatrix} a_m^i \\ p_m^i \end{bmatrix} = \begin{bmatrix} \frac{\mu_M}{\beta} p_m^e + a_m^e \\ -\frac{\mu_M}{\mu_I} p_m^e \end{bmatrix} \tag{28}$$

where a_0^i, p_0^i, a_m^i and p_m^i are the Fourier coefficients of boundary densities for the inclusion. Then, we can obtain the series-form Green's function for the matrix by applying Eq. (9) as shown below:

$$\begin{aligned} G(x,\xi) = & -\frac{\pi a}{2}[a_0^e k_M J_0'(k_M a) + p_0^e J_0(k_M a)] \\ & [Y_0(k_M\rho) - iJ_0(k_M\rho)] \\ & -\frac{\pi a}{2}\sum_{m=1}^{\infty}[a_m^e k_M J_m'(k_M a) + p_m^e J_m(k_M a)] \\ & [Y_m(k_M\rho) - iJ_m(k_M\rho)]\cos(m\phi) \\ & -\frac{p}{4\mu_M}[Y_0(k_M r) - iJ_0(k_M r)], \quad a \le \rho < \infty \end{aligned} \tag{29}$$

If we expand the fundamental function, we have

$$\begin{aligned} G(x,\xi) = & -\frac{\pi a}{2}[a_0^e k_M J_0'(k_M a) + p_0^e J_0(k_M a)] \\ & [Y_0(k_M\rho) - iJ_0(k_M\rho)] \\ & -\frac{\pi a}{2}\sum_{m=1}^{\infty}[a_m^e k_M J_m'(k_M a) + p_m^e J_m(k_M a)] \\ & [Y_m(k_M\rho) - iJ_m(k_M\rho)]\cos(m\phi) \\ & -\frac{p}{4\mu_M}\Big\{J_0(k_M e)[Y_0(k_M\rho) - iJ_0(k_M\rho)] \\ & +2\sum_{m=1}^{\infty} J_m(k_M e)[Y_m(k_M\rho) - iJ_m(k_M\rho)]\cos(m\phi)\Big\} \\ & e \le \rho < \infty \end{aligned} \tag{30}$$

$$\begin{aligned} G(x,\xi) = & -\frac{\pi a}{2}[a_0^e k_M J_0'(k_M a) + p_0^e J_0(k_M a)] \\ & [Y_0(k_M\rho) - iJ_0(k_M\rho)] \\ & -\frac{\pi a}{2}\sum_{m=1}^{\infty}[a_m^e k_M J_m'(k_M a) + p_m^e J_m(k_M a)] \\ & [Y_m(k_M\rho) - iJ_m(k_M\rho)]\cos(m\phi) \\ & -\frac{p}{4\mu_M}\Big\{J_0(k_M\rho)[Y_0(k_M e) - iJ_0(k_M e)] \\ & +2\sum_{m=1}^{\infty} J_m(k_M\rho)[Y_m(k_M e) - iJ_m(k_M e)]\cos(m\phi)\Big\} \\ & a \le \rho < e \end{aligned} \tag{31}$$

2.4 Linear algebraic equation

By moving the null-field point x_j to the jth circular boundary in the limit sense for Eq. (11), we have the linear algebraic equation

$$[\mathbf{U}]\{\mathbf{t}\} = [\mathbf{T}]\{\mathbf{u}\} + \{\mathbf{b}\} \tag{32}$$

where $\{\mathbf{b}\}$ is the vector due to the source of Green's function, $[\mathbf{U}]$ and $[\mathbf{T}]$ are the influence matrices with a dimension of $(N+1)(2M+1)$ by $(N+1)(2M+1)$, $\{\mathbf{u}\}$ and $\{\mathbf{t}\}$ denote the column vectors of Fourier coefficients with a dimension of $(N+1)(2M+1)$ by 1 in which $[\mathbf{U}]$, $[\mathbf{T}]$, $\{\mathbf{u}\}$, $\{\mathbf{t}\}$ and $\{\mathbf{b}\}$ can be defined as follows:

$$\begin{aligned} [\mathbf{U}] &= \begin{bmatrix} \mathbf{U}_{00} & \mathbf{U}_{01} & \cdots & \mathbf{U}_{0N} \\ \mathbf{U}_{10} & \mathbf{U}_{11} & \cdots & \mathbf{U}_{1N} \\ \vdots & \vdots & \ddots & \vdots \\ \mathbf{U}_{N0} & \mathbf{U}_{N1} & \cdots & \mathbf{U}_{NN} \end{bmatrix}, \\ [\mathbf{T}] &= \begin{bmatrix} \mathbf{T}_{00} & \mathbf{T}_{01} & \cdots & \mathbf{T}_{0N} \\ \mathbf{T}_{10} & \mathbf{T}_{11} & \cdots & \mathbf{T}_{1N} \\ \vdots & \vdots & \ddots & \vdots \\ \mathbf{T}_{N0} & \mathbf{T}_{N1} & \cdots & \mathbf{T}_{NN} \end{bmatrix} \end{aligned} \tag{33}$$

$$\{\mathbf{u}\} = \begin{Bmatrix} \mathbf{u}_0 \\ \mathbf{u}_1 \\ \mathbf{u}_2 \\ \vdots \\ \mathbf{u}_N \end{Bmatrix}, \quad \{\mathbf{t}\} = \begin{Bmatrix} \mathbf{t}_0 \\ \mathbf{t}_1 \\ \mathbf{t}_2 \\ \vdots \\ \mathbf{t}_N \end{Bmatrix}, \{\mathbf{b}\} = \begin{Bmatrix} \mathbf{b}_0 \\ \mathbf{b}_1 \\ \mathbf{b}_2 \\ \vdots \\ \mathbf{b}_N \end{Bmatrix} \tag{34}$$

where the vectors $\{\mathbf{u}_k\}$ and $\{\mathbf{t}_k\}$ are in the form of $\{a_0^k \;\; a_1^k \;\; b_1^k \;\; \cdots \;\; a_M^k \;\; b_M^k\}^T$ and $\{p_0^k \;\; p_1^k \;\; q_1^k \;\; \cdots \;\; p_M^k \;\; q_M^k\}^T$ respectively; the first subscript "j" ($j = 0,1,2,\ldots,N$) in $[\mathbf{U}_{jk}]$ and $[\mathbf{T}_{jk}]$ denotes the index of the j^{th} circle where the collocation point is located and the second subscript"k" ($k = 0,1,2,\cdots,N$) denotes the index of the k^{th} circle where boundary data $\{\mathbf{u}_k\}$ or $\{\mathbf{t}_k\}$ are specified, N is the number of circular holes in the domain and M indicates the truncated terms of Fourier series. The coefficient matrix of the linear algebraic system is partitioned into blocks, and each off-diagonal block corresponds to the influence matrices between two different circular cavities. The diagonal blocks are the influence matrices due to itself in each individual hole. After

uniformly collocating the point along the k^{th} circular boundary, the submatrix can be written as

$$\left[\mathbf{U}_{jk}\right] = \begin{bmatrix} U_{jk}^{0c}(\phi_1) & U_{jk}^{1c}(\phi_1) & U_{jk}^{1s}(\phi_1) \\ U_{jk}^{0c}(\phi_2) & U_{jk}^{1c}(\phi_2) & U_{jk}^{1s}(\phi_2) \\ U_{jk}^{0c}(\phi_3) & U_{jk}^{1c}(\phi_3) & U_{jk}^{1s}(\phi_3) \\ \vdots & \vdots & \vdots \\ U_{jk}^{0c}(\phi_{2M}) & U_{jk}^{1c}(\phi_{2M}) & U_{jk}^{1s}(\phi_{2M}) \\ U_{jk}^{0c}(\phi_{2M+1}) & U_{jk}^{1c}(\phi_{2M+1}) & U_{jk}^{1s}(\phi_{2M+1}) \end{bmatrix} \begin{bmatrix} \cdots & U_{jk}^{Mc}(\phi_1) & U_{jk}^{Ms}(\phi_1) \\ \cdots & U_{jk}^{Mc}(\phi_2) & U_{jk}^{Ms}(\phi_2) \\ \cdots & U_{jk}^{Mc}(\phi_3) & U_{jk}^{Ms}(\phi_3) \\ \ddots & \vdots & \vdots \\ \cdots & U_{jk}^{Mc}(\phi_{2M}) & U_{jk}^{Ms}(\phi_{2M}) \\ \cdots & U_{jk}^{Mc}(\phi_{2M+1}) & U_{jk}^{Ms}(\phi_{2M+1}) \end{bmatrix} \tag{35}$$

$$\left[\mathbf{T}_{jk}\right] = \begin{bmatrix} T_{jk}^{0c}(\phi_1) & T_{jk}^{1c}(\phi_1) & T_{jk}^{1s}(\phi_1) \\ T_{jk}^{0c}(\phi_2) & T_{jk}^{1c}(\phi_2) & T_{jk}^{1s}(\phi_2) \\ T_{jk}^{0c}(\phi_3) & T_{jk}^{1c}(\phi_3) & T_{jk}^{1s}(\phi_3) \\ \vdots & \vdots & \vdots \\ T_{jk}^{0c}(\phi_{2M}) & T_{jk}^{1c}(\phi_{2M}) & T_{jk}^{1s}(\phi_{2M}) \\ T_{jk}^{0c}(\phi_{2M+1}) & T_{jk}^{1c}(\phi_{2M+1}) & T_{jk}^{1s}(\phi_{2M+1}) \end{bmatrix} \begin{bmatrix} \cdots & T_{jk}^{Mc}(\phi_1) & T_{jk}^{Ms}(\phi_1) \\ \cdots & T_{jk}^{Mc}(\phi_2) & T_{jk}^{Ms}(\phi_2) \\ \cdots & T_{jk}^{Mc}(\phi_3) & T_{jk}^{Ms}(\phi_3) \\ \ddots & \vdots & \vdots \\ \cdots & T_{jk}^{Mc}(\phi_{2M}) & T_{jk}^{Ms}(\phi_{2M}) \\ \cdots & T_{jk}^{Mc}(\phi_{2M+1}) & T_{jk}^{Ms}(\phi_{2M+1}) \end{bmatrix} \tag{36}$$

$$\left\{\mathbf{b}_j\right\} = \begin{Bmatrix} \frac{-i\pi}{2} H_0^{(1)} k \left|\mathbf{x}(\rho_j,\phi_1) - \xi\right| \\ \frac{-i\pi}{2} H_0^{(1)} k \left|\mathbf{x}(\rho_j,\phi_2) - \xi\right| \\ \frac{-i\pi}{2} H_0^{(1)} k \left|\mathbf{x}(\rho_j,\phi_3) - \xi\right| \\ \vdots \\ \frac{-i\pi}{2} H_0^{(1)} k \left|\mathbf{x}(\rho_j,\phi_{2M+1}) - \xi\right| \end{Bmatrix} \tag{37}$$

where the influence coefficients are explicitly expressed as

$$U_{jk}^{nc}(\phi_m) = \int_{B_k} U(s_k, x_m)\cos(n\theta_k)\, R_k d\theta_k, \tag{38}$$

$$U_{jk}^{ns}(\phi_m) = \int_{B_k} U(s_k, x_m)\sin(n\theta_k)\, R_k d\theta_k, \tag{39}$$

$$T_{jk}^{nc}(\phi_m) = \int_{B_k} T(s_k, x_m)\cos(n\theta_k)\, R_k d\theta_k, \tag{40}$$

$$T_{jk}^{ns}(\phi_m) = \int_{B_k} T(s_k, x_m)\sin(n\theta_k)\, R_k d\theta_k \tag{41}$$

where $n = 0,1,2,\cdots,M$, $m = 1,2,\cdots,2M+1$, and ϕ_m is the polar angle of the collocating points x_m along the boundary. By rearranging the known and unknown sets, the unknown Fourier coefficients are determined. Equation (11) can be calculated by employing the relations of trigonometric function and the orthogonal property in the real computation. Only the finite M terms are used in the Fourier expansion of boundary densities and kernels. After obtaining the unknown Fourier coefficients, we can obtain the interior potential by employing Eq. (9).

2.5 Derivation of the Green's function with several circular holes and inclusions

For the problems with inclusions, we can decompose into subsystems of matrix and inclusion after one taking free body on the interface. The problem subject to the concentrated load in the matrix, we have

$$\left[U^M\right]\left\{t^M\right\} = \left[T^M\right]\left\{u^M\right\} + \{b\} \tag{42}$$

$$\left[U^I\right]\left\{t^I\right\} = \left[T^I\right]\left\{u^I\right\} \tag{43}$$

The problem subject to the concentrated load in the inclusion is shown below

$$\left[U^M\right]\left\{t^M\right\} = \left[T^M\right]\left\{u^M\right\} \tag{44}$$

$$\left[U^I\right]\left\{t^I\right\} = \left[T^I\right]\left\{u^I\right\} + \{b\} \tag{45}$$

where the superscripts "M" and "I" denote the systems of matrix and inclusion, respectively. Similarly, interface conditions of Eq. (5) can be rewritten as

$$t^I = \frac{\beta}{\mu_I}(u^M - u^I), \quad \text{n the interface} \tag{46}$$

$$-\mu_M t^M = \mu_I t^I, \quad \text{on the interface} \tag{47}$$

By assembling the matrices in Eqs. (42), (43), (46) and (47), we have

$$\begin{bmatrix} T_{11}^M & -U_{11}^M & 0 & 0 \\ 0 & 0 & T_{11}^I & -U_{11}^I \\ 0 & \mu_M & 0 & \mu_I \\ \beta & \mu_M & -\beta & 0 \end{bmatrix} \begin{bmatrix} u_1^M \\ t_1^M \\ u_1^I \\ t_1^I \end{bmatrix} = \begin{bmatrix} \frac{p}{\mu_M} U(\xi, x) \\ 0 \\ 0 \\ 0 \end{bmatrix} \quad (48)$$

By assembling the matrices in Eqs. (44), (45), (46) and (47), we have

$$\begin{bmatrix} T_{11}^M & -U_{11}^M & 0 & 0 \\ 0 & 0 & T_{11}^I & -U_{11}^I \\ 0 & \mu_M & 0 & \mu_I \\ \beta & \mu_M & -\beta & 0 \end{bmatrix} \begin{bmatrix} u_1^M \\ t_1^M \\ u_1^I \\ t_1^I \end{bmatrix} = \begin{bmatrix} 0 \\ \frac{p}{\mu_M} U(\xi, x) \\ 0 \\ 0 \end{bmatrix} \quad (49)$$

The unknown coefficients in the algebraic system can be determined. Then, we can solve the potential by Eq. (9). A general-purpose program for deriving the Green's function of Helmholtz problems with arbitrary number of circular holes and/or inclusions of arbitrary radii and various positions involving the Dirichlet or the Neumann or mixed boundary condition was developed.

3 Illustrative examples and discussions

Case 1: one inclusion in the matrix with a concentrated force

Following the same example of Wang and Sudak [Wang and Sudak (2007)], we suppose that $\mu_I = 4\mu_M$, $c_I = 2c_M$, and e is located at $1.1a$ on the x axis as shown Fig. 1(a). For the static case $(k = 0)$, we can replace the $H_0^{(1)}(kr)$ by $\ln r$ and redo the procedure. The formulation can be found in the Appendix A. On the other hand, the static solution by using the limiting process $(k \to 0)$ is also derived in the Appendix B. The stress σ_{zr}^* along the circular boundary is shown in Fig. 2(a). In the real implementation, direct substitution of zero k value yields the singular behavior in our formulation of Hankel function and can not be carried out in the program. We select $ka = 0.01$ to simulate the quasi-static result. Good agreement is made in Fig. 2(b) after comparing with that of Fig. 2(a). Parameter study of β on the stress σ_{zr}^* along the circular boundary is done as shown in Fig. 3(a). To simulate the ideally bonded case, we choose $\beta = 10^{32}$ in the real computation. Good agreement is made after comparing with that of the ideally bonded case $(\beta = \infty)$. The derivation of ideally bonded case is also given in the Appendix C. Figs. 3(a) and 3(b) show that the higher the λ value is, the larger the stress appears. Our results also match well with those of Wang and Sudak's data. Furthermore, test of convergence for the Fourier series using Parseval's sum are shown in Figs. 4(a) and 4(b). Figs. 5(a) and 5(b) show the distribution of displacement $(u_I^* = \mu_M |u_I| / p)$ along the circular boundary versus the wave number with $\lambda = 1$ by using the Wang and Sudak's approach and our method, respectively. Good agreement is made. It is expected that higher wave number yield higher oscillation along the angle from $0 \sim 2\pi$.

Case 2: infinite matrix with a single inclusion subject to a concentrated force

We also suppose the same parameters of $\mu_I = 4\mu_M$ and $c_I = 2c_M$ as the case 1. Here, the source is located at $e = 0.9a$ in the inclusion as shown in Fig. 1(b). To verify the accuracy of the present solution, we compare with the quasi-static result $(k_M a = 0.01)$ for the stress distribution along the interface as shown in Fig. 6 using the static solution $(k_M = 0)$ as derived in the Appendix A. Also, an alternative method by limiting the process $(k \to 0)$ is also given in the Appendix B. Regarding the series solution as well as the closed-form solution for the static case, the result is summarized in the Table 1. Excellent agreement between the two results is observed from the Fig. 6. The stress σ_{zr}^* versus $k_M a$ for different values of λ is shown in Fig. 7. Some amplifications for certain values of $k_M a$ can be found in the same trend of Fig. 3(b). Fig. 8 shows the distribution of displacement $(u_I^* = \mu_M |u_I| / p)$ along the circular

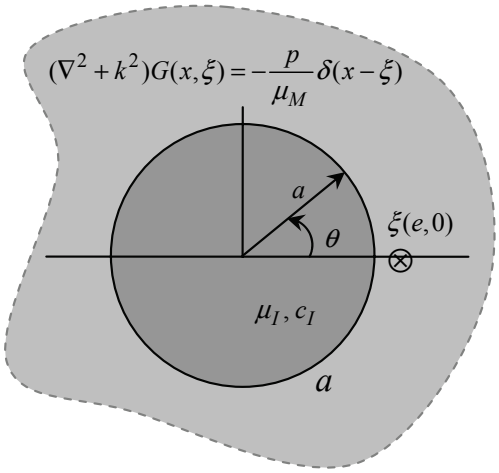

Figure 1(a): An infinite matrix containing a circular inclusion with a concentrated force at ξ in the matrix

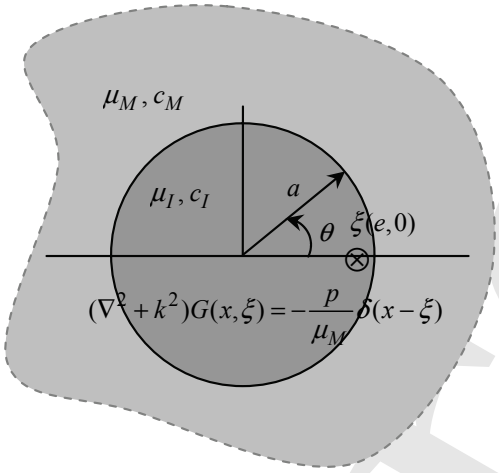

Figure 1(b): An infinite matrix containing a circular inclusion with a concentrated force at ξ in the inclusion

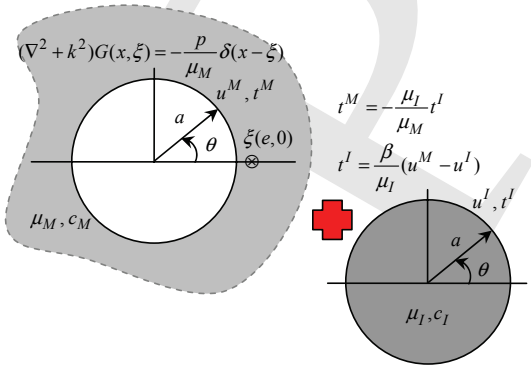

Figure 1(c): An infinite matrix containing a circular inclusion with a concentrated force at ξ in the matrix (take free body)

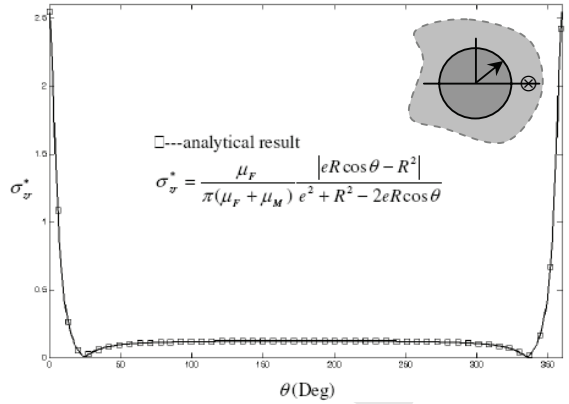

Figure 2(a): Distribution of σ^*_{zr} for the dynamic $(k_M a = 0.01)$ solution along the circular boundary (Wang and Sudak's solution)

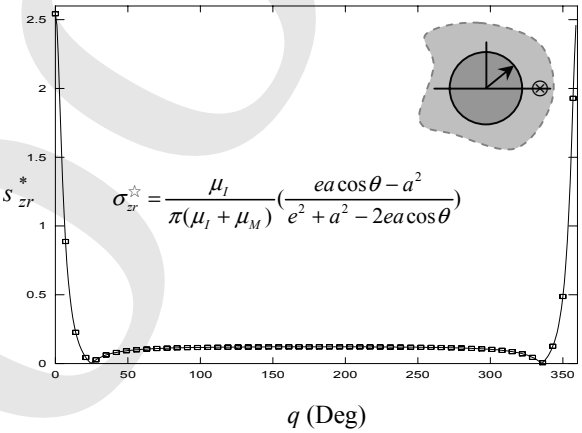

Figure 2(b): Distribution of σ^*_{zr} for the dynamic $(k_M a = 0.01)$ solution along the circular boundary by using the present solution

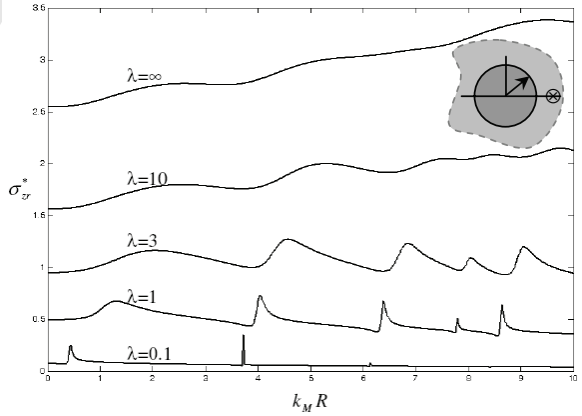

Figure 3(a): Parameter study of $\lambda = a\beta/\mu_M$ for the stress response (Wang and Sudak's solution)

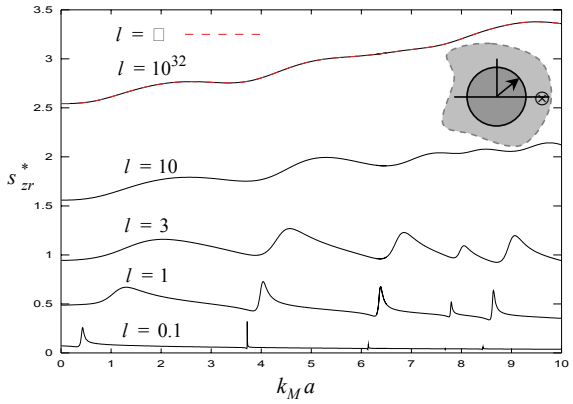

Figure 3(b): Parameter study of $\lambda = a\beta/\mu_M$ for the stress response by using the present solution

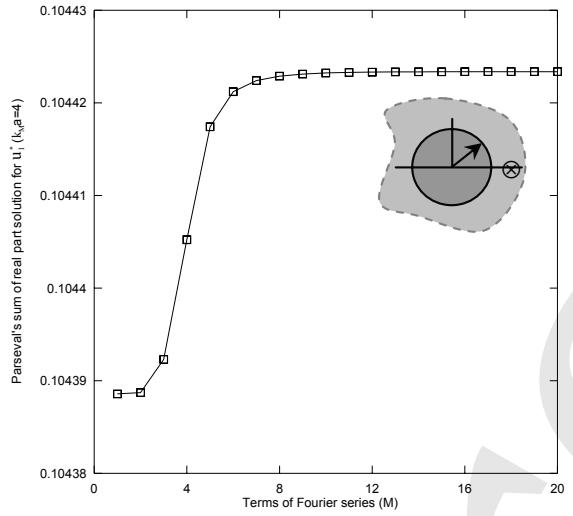

Figure 4(a): Test of convergence for Fourier series with a concentrated force in the matrix (real part)

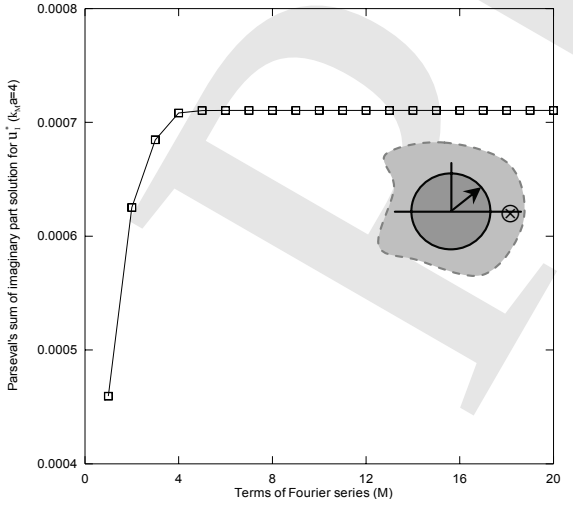

Figure 4(b): Test of convergence for Fourier series with a concentrated force in the matrix (imaginary part)

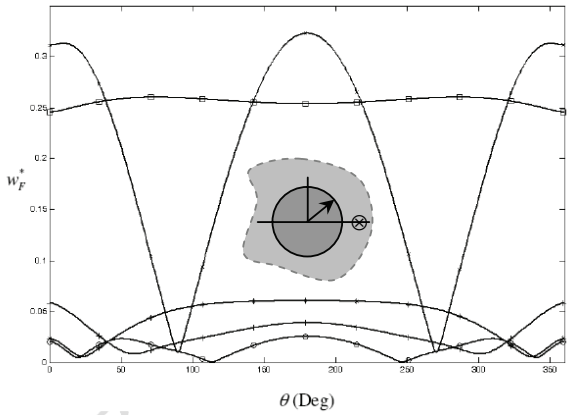

Figure 5(a): The distribution of displacement u_I^* along the circular boundary for the case of $\lambda = 1$ ($k_M a = 1,2,3,4,5$) (Wang and Sudak's solution)

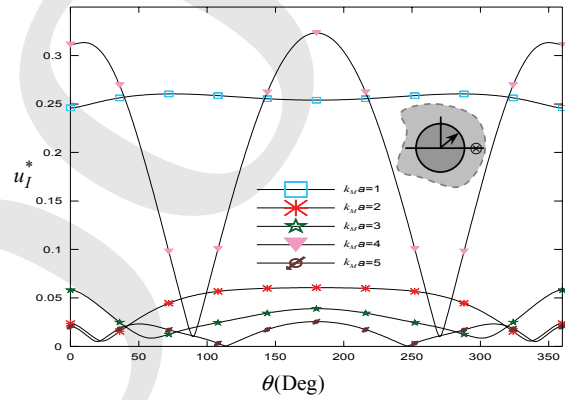

Figure 5(b): The distribution of displacement u_I^* along the circular boundary for the case of $\lambda = 1$ ($k_M a = 1,2,3,4,5$) by using the present solution

boundary versus the wave number with $\lambda = 1$.

Case 3: two inclusions in the matrix with a concentrated force

Following the success of the single-inclusion case to compare well with the Wang and Sudak's result, we extend to two inclusions as shown in Fig. 9. We also suppose the same properties of $\mu_I = 4\mu_M$ and $c_I = 2c_M$ as the case 1. Here, the concentrated source is located in the matrix of $e = (2.5, 0)$.Figure 10 shows the variation of $\sigma_{zr}^* = R\left|\sigma_{zr}^I\right|/p$ at the point $(-a_1, \pi)$ for various distances $d = 0.01 \sim 13$.The local maximum or minimum of σ_{zr}^* occurs in a period of half wavelength. The contour of the displacement for the

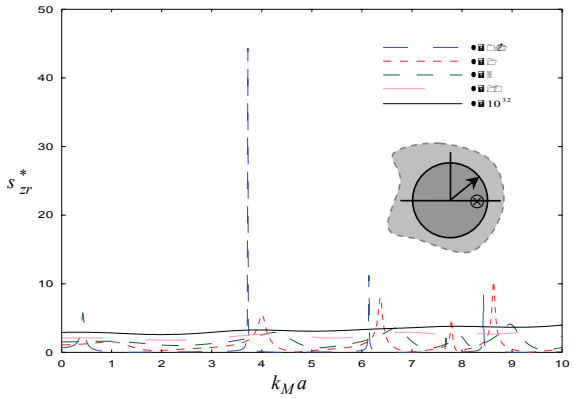

Figure 6: Distribution of σ^*_{zr} for the dynamic $(k_M a = 0.01)$ solution along the circular boundary $(e = 0.9a)$

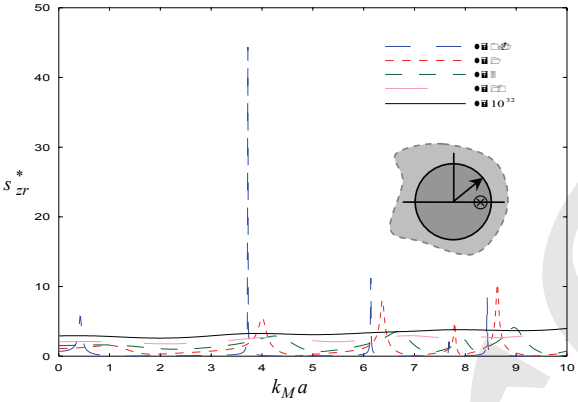

Figure 7: Parameter study of $\lambda = a\beta/\mu_M$ for the stress response $(e = 0.9a)$

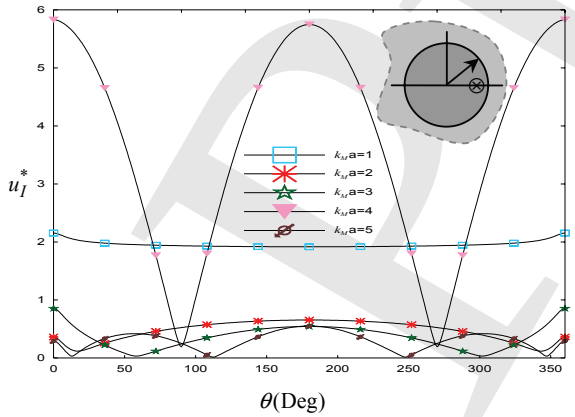

Figure 8: The distribution of displacement u^*_I along the circular boundary for the case of $\lambda = 1$ $(k_M a = 1,2,3,4,5)$ $(e = 0.9a)$

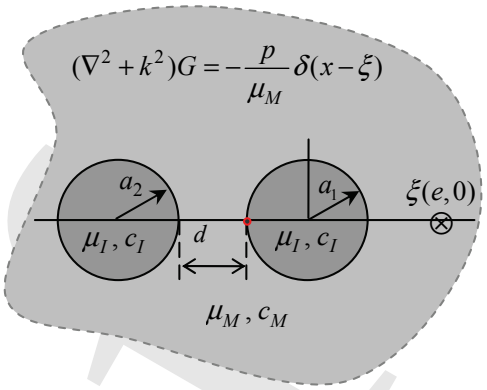

Figure 9: An infinite matrix containing two circular inclusions with a concentrated force at ξ in the matrix

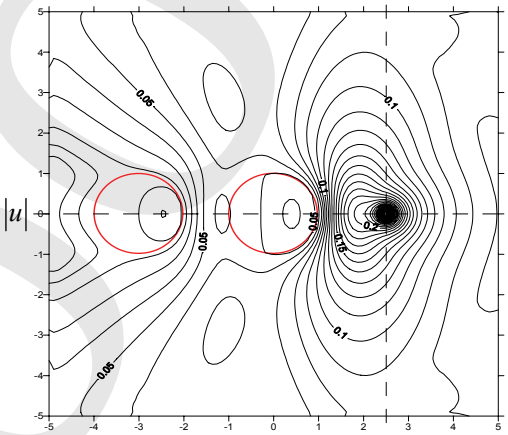

Figure 10: Distribution of σ^*_{zr} of the matrix at the position of (a_1, π) various d

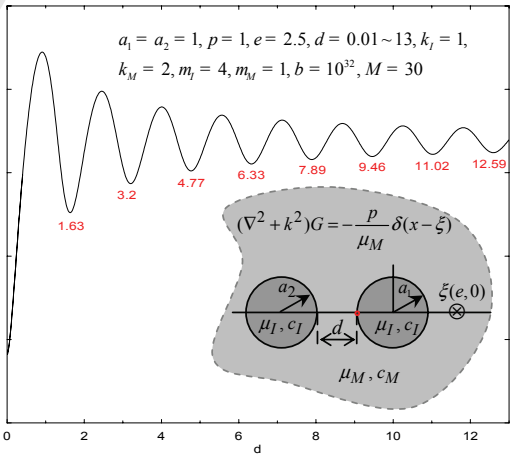

Figure 11: The contour of the displacement for an infinite matrix containing two inclusions with a concentrated force at ξ in the matrix

two-inclusions problem is shown in Fig. 11.

4 Conclusions

Two-dimensional antiplane dynamic Green's functions for a circular inclusion or two circular inclusions with imperfect interface have been successfully derived by using the present formulation. A limiting case of zero wave number matches well with the static solution. Ideally bonded case can be seen as a special case of our solution. Moreover, good agreement is made after comparing with the analytical solution derived by Wang and Sudak's results. Parameter study of wave number and interface constant is also done. Following the success of two-dimensional antiplane dynamic Green's functions, it is straightforward to extend to solve screw dislocation problems [Fan and Wang (2003)].

References

Ang, W. T. (1987): A boundary integral equation for deformations of an elastic body with an arc crack. *Quarterly of Applied Mathematics*, vol. 45, pp. 131-139.

Ang, W. T.; Choo, K. K.; Fan, H. (2004): A Green's function for steady-state two-dimensional isotropic heat conduction across a homogeneously imperfect interface. *Communications in Numerical Methods in Engineering*, vol. 20, pp. 391-399.

Ang, W. T.; Fan, H. (2004): A hypersingular boundary integral method for quasi-static antiplane deformations of an elastic bimaterial with an imperfect and visco-elastic interface. *Engineering Computations*, vol. 21, pp. 529-539.

Ang, W. T.; Telles, J. C. F. (2004): A numerical Green's function for multiple cracks in anisotropic bodies. *Journal of Engineering Mathematics*, vol. 49, pp. 197-207.

Chen, J. T.; Ke, J. N.; Liao, H. Z. (2007): Construction of Green's function using null-field integral approach for Laplace problems with circular boundaries. *CMC: Computers, Materials & Continua*, Accepted.

Chen, J. T.; Liu, L. W.; Hong, H. K. (2003): Spurious and true eigensolutions of Helmholtz BIEs and BEMs for a multiply connected problem. *Proceedings of the Royal Society* Series A, vol. 459, pp. 1891-1924.

Chen, J. T.; Shen, W. C.; Chen, P. Y. (2006): Analysis of circular torsion bar with circular holes using null-field approach. *CMES: Computer Modeling in Engineering Science*, vol. 12, pp. 109-119.

Chen, J. T.; Wu, A. C. (2006): Null-field approach for piezoelectricity problems with arbitrary circular inclusions. *Engineering Analysis with Boundary Elements*, vol. 30, pp. 971-993.

Chen, T. (2001): Thermal conduction of a circular inclusion with variable interface parameter. *Int. J. Solids Struct.*, vol. 38, pp. 3081-3097.

Cheng, Z. Q.; Batra, R. C. (1999): Exact Eshelby tensor for a dynamic circular cylindrical inclusion. *ASME J. Appl. Mech.*, vol. 66, pp. 563-565.

Denda, M.; Araki, Y.; Yong, Y. K. (2004): Time-harmonic BEM for 2-D piezoelectricity applied to eigenvalue problem. *Int. J. Solids & Struct.*, vol. 41, pp. 7241-7265.

Denda, M.; Wang, C. Y.; Yong, Y. K. (2003): 2-D time-harmonic BEM for solids of general anisotrophy with application to eigenvalue problems. *J. Sound Vibrat.*, vol. 261, pp. 247-276.

Fan, H.; Wang, G. F. (2003): Screw dislocation interacting with an imperfect interface, *Mechanics of Materials*, vol. 35 pp. 943-953.

Hashin, Z. (1991): The spherical inclusion with imperfect interface. *ASME J. Appl. Mech.*, vol. 12, pp. 444-449.

Hwu, C. B.; Yen, W. J. (1991): Green functions of 2-dimensional anisotropic plates containing an elliptic hole. *International J of Solids Structures*, vol. 27, pp. 1705-1719.

Kitahara, M. (1985): Boundary integral equation methods in eigenvalue problems of elastodynamics and thin plates. Elsevier, Amsterdam.

Michelitsch, T. M.; Levin, V. M.; Gao, H. J. (2002): Dynamic potentials and Green's functions of a quasi-plane piezoelectric medium with inclusion. *Proc. R. Soc. Lond.*, vol. A458, pp.

2393-2415.

Mikata, Y.; Nemat-Nasser, S. (1990): Elastic field due to a dynamically transforming spherical inclusion. *ASME J. Appl. Mech.*, vol. 57, pp. 845-849.

Mura, T. (1988): Inclusion problems. *ASME Applied Mechanics Reviews*, vol. 41, pp. 15-20.

Mura, T.; Shodja, H. M.; Hirose, Y. (1996): Inclusion problems. *ASME Applied Mechanics Reviews*, vol. 49, pp. S118-S127.

Ru, C. Q.; Schiavone, P. (1997): A circular inclusion with circumferentially inhomogeneous interface in antiplane shear. *Proc. R. Soc. Lond.*, vol. A 453, pp. 2551-2572.

Talbot, D. R. S.; Willis, J. R. (1983): Variational estimates for dispersion and attenuation of waves in random composite III. Fiber-reinforced materials. *Int. J. Solids & Struct.*, vol. 19, pp. 793-811.

Wang, X.; Sudak, L. J. (2007): Antiplane time-harmonic Green's functions for a circular inhomogeneity with an imperfect interface. *Mech. Res. Commun.*, Accepted.

Wang, X.; Zhong, Z. (2003): Two-dimensional time-harmonic dynamic Green's functions in transversely isotropic piezoelectric solids. *Mech. Res. Commun.*, vol. 30, pp. 589-593.

Wang, X. D.; Meguid, S. A. (1999): Dynamic interaction between a matrix crack and a circular inhomogeneity with a distinct interphase. *Int. J. Solids & Struct.*, vol. 36, pp. 517-531.

Willis, J. R. (1980a): A polarization approach to the scattering of elastic waves I. scattering by a single inclusion. *J. Mech. Phys. Solids*, vol. 28, pp. 287-305.

Willis, J. R. (1980b): A polarization approach to the scattering of elastic waves II. multiple scattering from inclusions. *J. Mech. Phys. Solids*, vol. 28, pp. 307-327.

Wu, K. C.; Chen, S. H. (2007)**:** Two dimensional dynamic Green's functions for piezoelectric materials. *CMES: Computer Modeling in Engineering & Sciences*, vol. 20, no. 3, pp. 147-156.

Yang, B.; Tewary, V. K. (2006): Efficient Green's function modeling of line and surface defects in multilayered anisotropic elastic and piezoelectric materials. *CMES: Computer Modeling in Engineering & Sciences*, Vol. 15, No. 3, pp. 165-178.

Chen, J. T.; Chou, K. S. (2007): Three ways for calculating circular boundary integrals, *Math. Media*, Accepted (in Chinese).

Appendix A Static cases

Case 1: a concentrated force in the matrix

For the static case ($k=0$) and ideally bonded interface ($\beta \to \infty$), we can replace the $H_0^1(kr)$ by $\ln r$ and redo the procedure. Then, we follow the formulation for Laplace problems in [Chen, Ke and Liao (2007)]. For the problem with an inclusion, we can decompose into subsystems of the matrix and inclusion after taking free body on the interface as shown in Fig. 1(c). Then, by collocating x on (a^-,ϕ) and (a^+,ϕ) for the matrix and inclusion, respectively, the null-field equations yield

$$0 = -2\pi a_0^e - \sum_{m=1}^{\infty} \pi (a_m^e \cos m\phi + b_m^e \sin m\phi)$$
$$- 2\pi a \ln a p_0^e + \sum_{m=1}^{\infty} \frac{a\pi}{m} (p_m^e \cos m\phi + p_m^e \sin m\phi)$$
$$- \frac{p}{\mu_M} [\ln e - \sum_{m=1}^{\infty} \frac{1}{m} (\frac{a}{e})^m \cos(m\phi)]$$
$$x \to (a^-,\phi) \quad \text{(A1)}$$

$$0 = -\sum_{m=1}^{\infty} \pi (a_m^i \cos m\phi + b_m^i \sin m\phi) - 2\pi a \ln a p_0^i$$
$$+ \sum_{m=1}^{\infty} \frac{a\pi}{m} (p_m^i \cos m\phi + q_m^i \sin m\phi)$$
$$x \to (a^+,\phi) \quad \text{(A2)}$$

Similarly, interface conditions of Eq. (5) can be rewritten as

$$t^I = \frac{\beta}{\mu_I}(u^M - u^I), \quad \text{on the interface} \quad \text{(A3)}$$
$$-\mu_M t^M = \mu_I t^I, \quad \text{on the interface} \quad \text{(A4)}$$

By assembling the matrices in Eqs. (A1), (A2),

(A3) and (A4), we have

$$\begin{bmatrix} T_{11}^M & -U_{11}^M & 0 & 0 \\ 0 & 0 & T_{11}^I & -U_{11}^I \\ 0 & \mu_M & 0 & \mu_I \\ \beta & \mu_M & -\beta & 0 \end{bmatrix} \begin{bmatrix} u_1^M \\ t_1^M \\ u_1^I \\ t_1^I \end{bmatrix} = \begin{bmatrix} \frac{p}{\mu_M} U(\xi,x) \\ 0 \\ 0 \\ 0 \end{bmatrix} \quad \text{(A5)}$$

After rearranging Eq. (A5), we have

$$\begin{bmatrix} T_{11}^M & -U_{11}^M \\ T_{11}^I & \frac{\mu_M}{\beta} T_{11}^I + \frac{\mu_M}{\mu_I} U_{11}^I \end{bmatrix} \begin{bmatrix} u_1^M \\ t_1^M \end{bmatrix} = \begin{bmatrix} \frac{p}{\mu_M} U(\xi,x) \\ 0 \end{bmatrix} \quad \text{(A6)}$$

The unknown coefficients in the algebraic system can be determined as shown below:

$$\begin{bmatrix} a_0^e \\ a_m^e \\ b_m^e \\ p_0^e \\ p_m^e \\ q_m^e \end{bmatrix} = \begin{bmatrix} -\frac{p}{2\pi\mu_M} \ln e \\ \frac{p(\beta a + m\mu_I)}{m\pi[m\mu_M\mu_I + \beta a(\mu_M+\mu_I)]} (\frac{a}{e})^m \\ 0 \\ 0 \\ -\frac{p\beta\mu_I}{\mu_M\pi[m\mu_M\mu_I + \beta a(\mu_M+\mu_I)]} (\frac{a}{e})^m \\ 0 \end{bmatrix} \quad \text{(A7)}$$

where a_0^e, p_0^e, a_m^e and p_m^e, $m = 1,2,3,\ldots$ are the Fourier coefficients of boundary densities for the matrix. As β approaches infinity, we have

$$\begin{bmatrix} a_0^e \\ a_m^e \\ b_m^e \\ p_0^e \\ p_m^e \\ q_m^e \end{bmatrix} = \begin{bmatrix} -\frac{p}{2\pi\mu_M} \ln e \\ \frac{p}{m\pi(\mu_M+\mu_I)} (\frac{a}{e})^m \\ 0 \\ 0 \\ -\frac{p\mu_I}{a\mu_M\pi(\mu_M+\mu_I)} (\frac{a}{e})^m \\ 0 \end{bmatrix} \quad \text{(A8)}$$

Then, we can obtain the analytical result for the static stress $\sigma_{zr} = \frac{\mu_I}{\pi(\mu_I+\mu_M)} \sum_{m=1}^{\infty} a_m \cos(m\theta)$ of the matrix as shown below:

$$\sigma_{zr} = \frac{a}{p}\sigma_{zr}^M = \frac{\mu_I}{\pi(\mu_I+\mu_M)} \sum_{m=1}^{\infty} (\frac{a}{e})^m \cos m\theta, \quad e > a \quad \text{(A9)}$$

The Wang and Sudak's closed-form solution is shown below:

$$\sigma_{zr} = \frac{\mu_I}{\pi(\mu_I+\mu_M)} \left(\frac{ea\cos\theta - a^2}{e^2 + a^2 - 2ea\cos\theta} \right), \quad e > a \quad \text{(A10)}$$

By expanding the Eq. (A10) into Fourier series, we have

$$\sigma_{zr} = \frac{\mu_I}{\pi(\mu_I+\mu_M)} \sum_{m=1}^{\infty} a_m \cos(m\theta), \quad e > a \quad \text{(A11)}$$

where the Fourier coefficient of a_m can be determined by using the Poison integral formula [Chen and Chou (2007)] as shown below:

$$\begin{aligned} a_m &= \frac{1}{\pi} \int_0^{2\pi} (\frac{ea\cos\theta - a^2}{e^2 + a^2 - 2ea\cos\theta}) \cos(m\theta) d\theta \\ &= \frac{1}{\pi} \int_0^{2\pi} [\frac{(\frac{a}{e})\cos\theta - (\frac{a}{e})^2}{1 + (\frac{a}{e})^2 - 2(\frac{a}{e})\cos\theta}] \cos(m\theta) d\theta \\ &= \frac{2}{1-(\frac{a}{e})^2} \frac{(\frac{a}{e})^m - (\frac{a}{e})^{m+2}}{2} \\ &= (\frac{a}{e})^m, \\ & e > a \end{aligned} \quad \text{(A12)}$$

An alternative proof by using the degenerate kernel can also be obtained as shown below:

$$\begin{aligned} U(s,x) &= \ln\sqrt{e^2 + a^2 - 2ea\cos\theta} \\ &= \begin{cases} \ln e - \sum_{m=1}^{\infty} \frac{1}{m} (\frac{a}{e})^m \cos(m\theta), & e \geq a \\ \ln a - \sum_{m=1}^{\infty} \frac{1}{m} (\frac{e}{a})^m \cos(m\theta), & a > e \end{cases} \end{aligned} \quad \text{(A13)}$$

$$\begin{aligned} L(s,x) &= \frac{\partial U(s,x)}{\partial a} = \frac{a - e\cos\theta}{e^2 + a^2 - 2ea\cos\theta} \\ &= \begin{cases} -\sum_{m=1}^{\infty} (\frac{a^{m-1}}{e^m}) \cos(m\theta), & e > a \\ \frac{1}{a} + \sum_{m=1}^{\infty} (\frac{e^m}{a^{m+1}}) \cos(m\theta), & a > e \end{cases} \end{aligned} \quad \text{(A14)}$$

By multiplying $(-a)$ into Eq. (A14), we can also obtain the result of static case

$$\sigma_{zr} = \frac{\mu_I}{\pi(\mu_I+\mu_M)} \sum_{m=1}^{\infty} (\frac{a}{e})^m \cos(m\theta), \quad e > a \tag{A15}$$

Therefore, we have proved that our series-form solution is mathematically equivalent to the closed-form solution of Wang and Sudak.

Case 2: a concentrated force in the inclusion

Similarly as shown in the case 1, we can obtain the unknown coefficients as shown below:

$$\begin{bmatrix} a_0^e \\ a_m^e \\ b_m^e \\ p_0^e \\ p_m^e \\ q_m^e \end{bmatrix} = \begin{bmatrix} -\frac{p\mu_I}{2\pi\mu_M^2}\ln a \\ \frac{p\beta a\mu_I}{m\mu_M[a\pi\beta\mu_M+\pi\mu_I(a\beta+m\mu_M)]}(\frac{e}{a})^m \\ 0 \\ \frac{p\mu_I}{2a\pi\mu_M^2} \\ \frac{p\beta\mu_I}{\mu_M[a\pi\beta\mu_M+\pi\mu_I(a\beta+m\mu_M)]}(\frac{e}{a})^m \\ 0 \end{bmatrix} \tag{A16}$$

where a_0^e, p_0^e, a_m^e and p_m^e , $m = 1,2,3,\ldots$ are the Fourier coefficients of boundary densities for the inclusion. As β approaches infinity, we have

$$\begin{bmatrix} a_0^e \\ a_m^e \\ b_m^e \\ p_0^e \\ p_m^e \\ q_m^e \end{bmatrix} = \begin{bmatrix} -\frac{p\mu_I}{2\pi\mu_M^2}\ln a \\ \frac{p\mu_I}{m\mu_M\pi(\mu_M+\mu_I)}(\frac{e}{a})^m \\ 0 \\ \frac{p\mu_I}{2a\pi\mu_M^2} \\ \frac{p\mu_I}{\mu_M a\pi(\mu_M+\mu_I)}(\frac{e}{a})^m \\ 0 \end{bmatrix} \tag{A17}$$

Then, we can obtain the analytical result for the static stress $(\sigma_{zr} = a\sigma_{zr}^I/p = a\sigma_{zr}^M/p)$ of the inclusion as shown below:

$$\begin{aligned} \sigma_{zr} &= \frac{a}{p}\sigma_{zr}^M \\ &= \frac{\mu_I}{2\pi\mu_M} + \frac{\mu_I}{\pi(\mu_I+\mu_M)} \sum_{m=1}^{\infty} \left(\frac{e}{a}\right)^m \cos m\theta, \\ &\qquad a > e \end{aligned} \tag{A18}$$

A closed-form solution can be obtained by using the degenerate kernel. By multiplying (a) into Eq. (A14), we can also obtain the result of closed-form solution for the inclusion

$$\begin{aligned} \sigma_{zr} = &\frac{\mu_I}{\pi(\mu_I+\mu_M)} \left(\frac{a^2 - ea\cos\theta}{e^2+a^2-2ea\cos\theta}\right) \\ &+ \frac{1}{2\pi}\left(\frac{\mu_I^2-\mu_M\mu_I}{\mu_M^2+\mu_M\mu_I}\right), \quad a > e \end{aligned} \tag{A19}$$

Therefore, we have proved that the closed-form solution can be obtained mathematically by using the degenerate kernel. Based on the Fourier series expansion, the closed-form solution of Eq. (A19) yields

where the Fourier coefficient of a_0 and a_m can be determined by using the Poison integral formula as shown below:

$$\begin{aligned} a_m &= \frac{1}{\pi}\int_0^{2\pi} (\frac{a^2-ea\cos\theta}{e^2+a^2-2ea\cos\theta})\cos(m\theta)d\theta \\ &= \frac{1}{\pi}\int_0^{2\pi} [\frac{(\frac{a}{e})^2-(\frac{a}{e})\cos\theta}{1+(\frac{a}{e})^2-2(\frac{a}{e})\cos\theta}]\cos(m\theta)d\theta \\ &= \frac{2}{(\frac{a}{e})^2-1}\frac{(\frac{a}{e})^{-m+2}-(\frac{a}{e})^{-m}}{2} \\ &= (\frac{e}{a})^m, \\ &\quad a > e \end{aligned} \tag{A20}$$

$$\begin{aligned} a_0 &= \frac{1}{2\pi}\int_0^{2\pi} [\frac{\mu_I}{\pi(\mu_I+\mu_M)}(\frac{a^2-ea\cos\theta}{e^2+a^2-2ea\cos\theta}) \\ &+ \frac{1}{2\pi}(\frac{\mu_I^2-\mu_M\mu_I}{\mu_M^2+\mu_M\mu_I})]d\theta \\ &= \frac{1}{2\pi}\int_0^{2\pi} \frac{\mu_I}{\pi(\mu_I+\mu_M)}[\frac{(\frac{a}{e})^2-(\frac{a}{e})\cos\theta}{1+(\frac{a}{e})^2-2(\frac{a}{e})\cos\theta}]d\theta \\ &+ \frac{1}{2\pi}(\frac{\mu_I^2-\mu_M\mu_I}{\mu_M^2+\mu_M\mu_I}) \\ &= \frac{\mu_I}{\pi(\mu_I+\mu_M)}\frac{(\frac{a}{e})^2-1}{(\frac{a}{e})^2-1} + \frac{1}{2\pi}(\frac{\mu_I^2-\mu_M\mu_I}{\mu_M^2+\mu_M\mu_I}) \\ &= \frac{\mu_I}{2\pi\mu_M}, \\ &\quad a > e \end{aligned} \tag{A21}$$

It is straightforward to represent the closed-form solution into Fourier series solution. On the con-

trary, it always needs special treatment, e.g., Watson transformation if we would obtain the closed-form solution by way of Fourier series solution. Here, we do not employ the Watson transformation, but take advantage of expressions of degenerate kernels for the fundamental solution. The contours of shear stress $\sigma_{zx} = \sigma_{zr}\cos\phi - \sigma_{z\theta}\sin\phi$ and $\sigma_{zy} = \sigma_{zr}\sin\phi + \sigma_{z\theta}\cos\phi$ for a concentrated force in the matrix and inclusion are summarized in the Table 2 and 3, respectively.

$$\sigma_{zr} = a_0 + \frac{\mu_I}{\pi(\mu_I + \mu_M)} \sum_{m=1}^{\infty} a_m \cos(m\theta), \quad a > e \tag{A22}$$

Table 1: Series-form & closed-form solutions for the static case (ideally bonded interface)

	Concentrated force in the matrix	**Concentrated force in the inclusion**
Problem statement	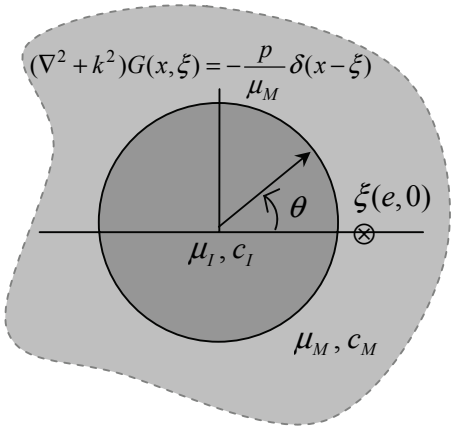	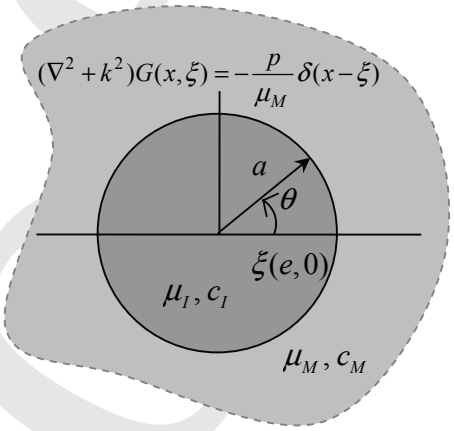
Stress distribution along the interface	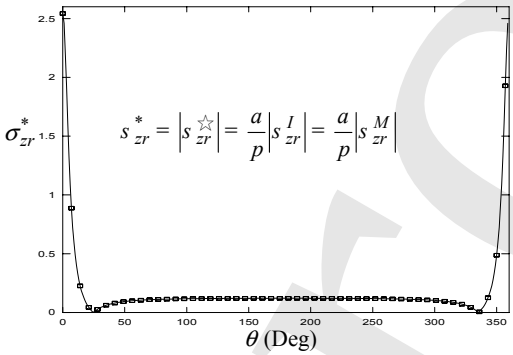	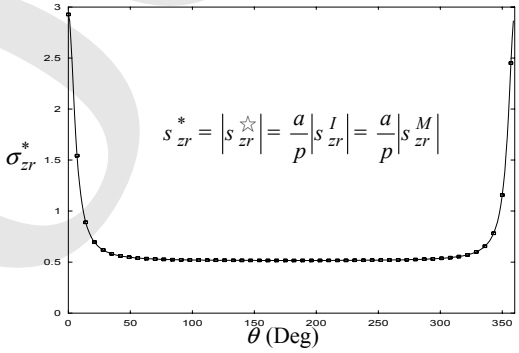
Closed-form solution	$\sigma^{\star}_{zr}=\frac{\mu_I}{\pi(\mu_I+\mu_M)}\left(\frac{ea\cos\theta-a^2}{e^2+a^2-2ea\cos\theta}\right)$ [Wang and Sudak, (2007)]	$\sigma^{\star}_{zr}=\frac{\mu_I}{\pi(\mu_I+\mu_M)}\left(\frac{a^2-ea\cos\theta}{e^2+a^2-2ea\cos\theta}\right)+\frac{1}{2\pi}\left(\frac{\mu_I^2-\mu_M\mu_I}{\mu_M^2+\mu_M\mu_I}\right)$
Seires-form solution	$\sigma^{\star}_{zr}=\frac{\mu_I}{\pi(\mu_I+\mu_M)}\sum_{m=1}^{\infty}\left(\frac{a}{e}\right)^m\cos m\theta$	$\sigma^{\star}_{zr}=\frac{\mu_I}{2\pi\mu_M}+\frac{\mu_I}{\pi(\mu_I+\mu_M)}\sum_{m=1}^{\infty}\left(\frac{e}{a}\right)^m\cos m\theta$

Table 2: Stress contours of σ_{zx} and σ_{zy} for the static and dynamic solutions (a concentrated force in the matrix)

Static case

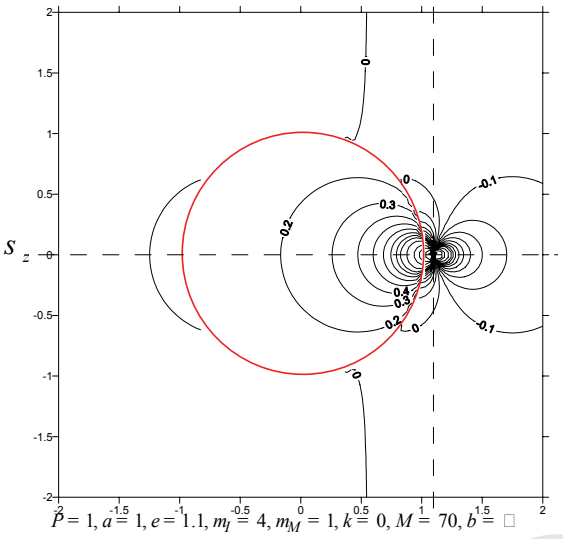

Contour of s_{zx}

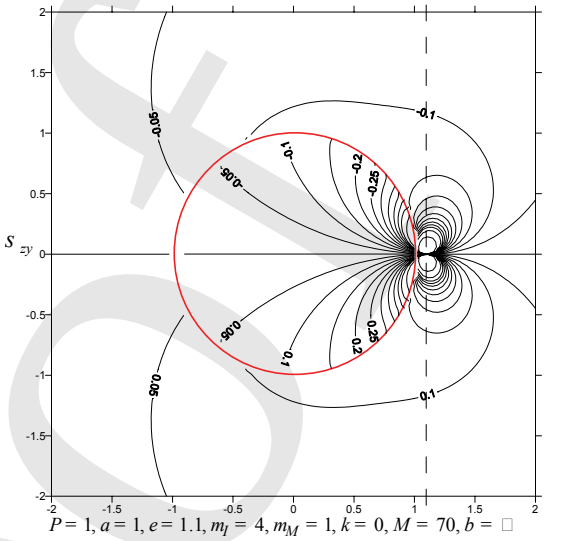

Contour of s_{zy}

Dynamic case

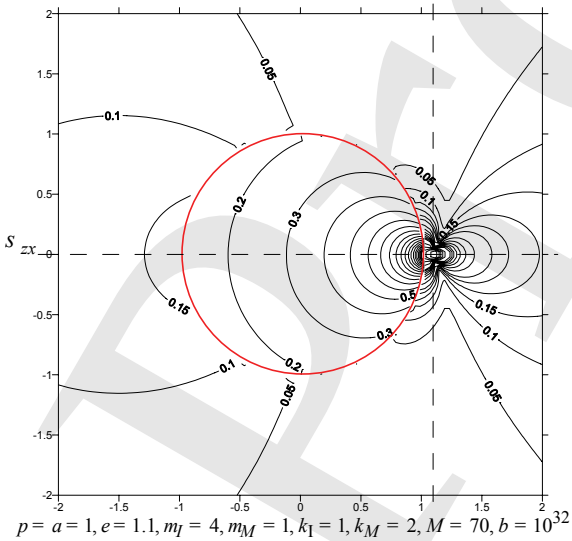

Contour of s_{zx}

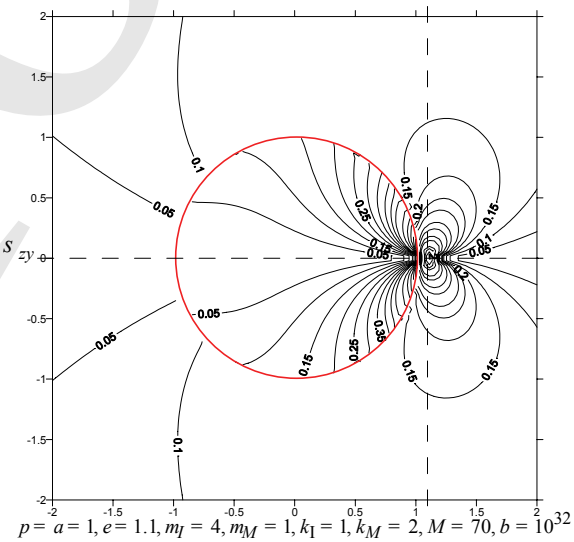

Contour of s_{zy}

Table 3: Stress contours of σ_{zx} and σ_{zy} for the static and dynamic solutions (a concentrated force in the inclusion)

Static case	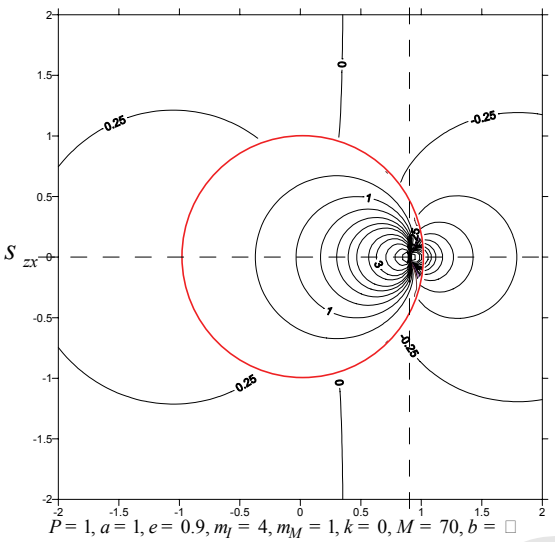 $P = 1, a = 1, e = 0.9, m_I = 4, m_M = 1, k = 0, M = 70, b =$ □	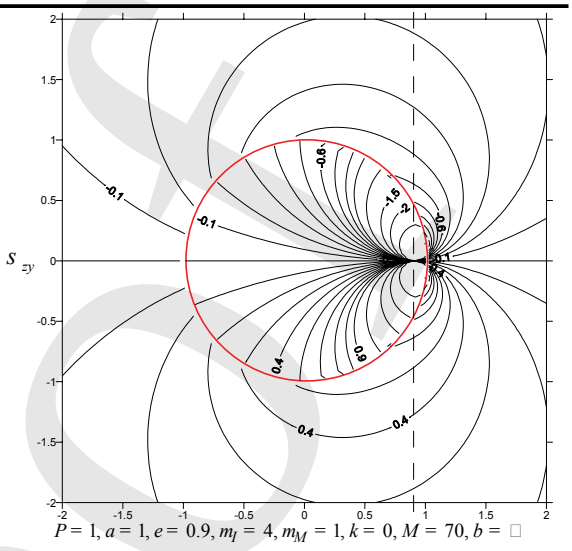 $P = 1, a = 1, e = 0.9, m_I = 4, m_M = 1, k = 0, M = 70, b =$ □
	Contour of s_{zx}	Contour of s_{zy}
Dynamic case	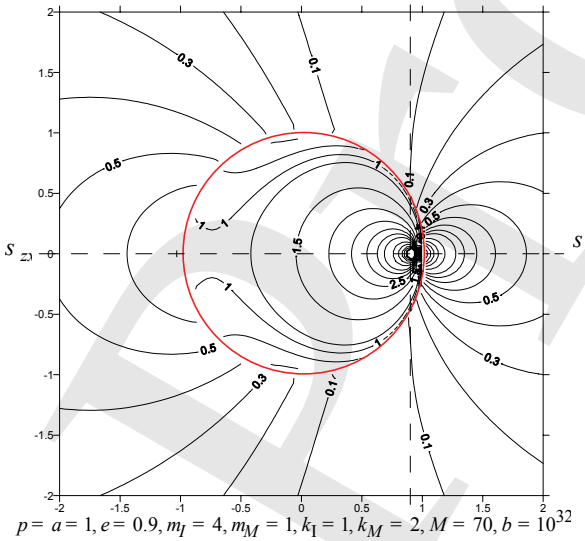 $p = a = 1, e = 0.9, m_I = 4, m_M = 1, k_I = 1, k_M = 2, M = 70, b = 10^{32}$	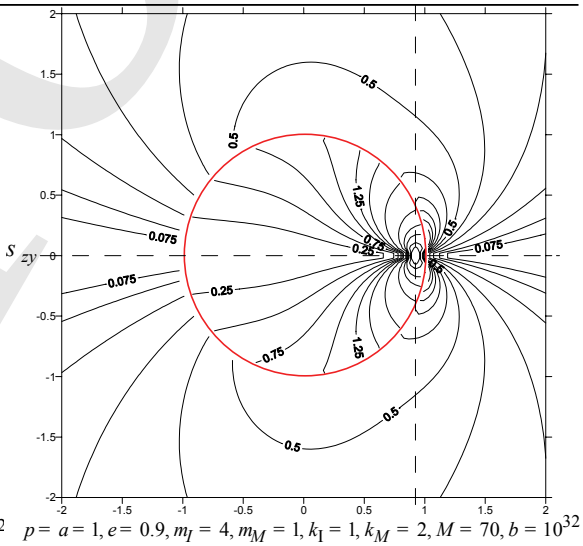 $p = a = 1, e = 0.9, m_I = 4, m_M = 1, k_I = 1, k_M = 2, M = 70, b = 10^{32}$
	Contour of s_{zx}	Contour of s_{zy}

Appendix B Derivation of the static solutions by using the limiting process $(k \to 0)$

Asymptotic formula	$z \to 0$	$z \to 0$
	$J_0(z) \sim 1$	$J_m(z) \sim (\frac{1}{2}z)^m / m!$
	$J_0'(z) \sim -(\frac{1}{2}z)$	$J_m'(z) \sim (\frac{1}{2}z)^{m-1} / 2(m-1)!$
	$Y_0(z) \sim (2/\pi)\ln z$	$Y_m(z) \sim -\frac{1}{\pi}(m-1)!(\frac{1}{2}z)^{-m}$
	$Y_0'(z) \sim \frac{1}{\pi}(\frac{1}{2}z)^{-1}$	$Y_m'(z) \sim \frac{m!}{2\pi}(\frac{1}{2}z)^{-m-1}$
Case 1	$s_{zr}^{\star} = \frac{a}{p}s_{zr}^{M} = -\frac{a}{p}m_M[p_0^e + \sum_{m=1}^{\infty} p_m^e \cos(mq)]$ for the ideally bonded interface and a concentrated force in the matrix	
Limiting process	$\lim_{b} p_0^e = \lim_{b} \frac{pbk_I m_I[J_0(k_M e) + iY_0(k_M e)]J_0'(k_I a)}{2pam_M\{k_I m_I J_0'(k_I a)[-b[J_0(k_M a) + iY_0(k_M a)] + k_M m_M[J_0'(k_M a) + iY_0'(k_M a)]] + bk_M m_M J_0(k_I a)[J_0'(k_M a) + iY_0'(k_M a)]\}}$	
	$= \frac{-pk_I m_I[J_0(k_M e) + iY_0(k_M e)]J_0'(k_I a)}{2pam_M\{k_I m_I J_0'(k_I a)[J_0(k_M a) + iY_0(k_M a)] - k_M m_M J_0(k_I a)[J_0'(k_M a) + iY_0'(k_M a)]\}}$	
	$\lim_{k\to 0} p_0^e = \lim_{k\to 0} \frac{-pk_I m_I[J_0(k_M e) + iY_0(k_M e)]J_0'(k_I a)}{2pam_M\{k_I m_I J_0'(k_I a)[J_0(k_M a) + iY_0(k_M a)] - k_M m_M J_0(k_I a)[J_0'(k_M a) + iY_0'(k_M a)]\}}$	
	$= \lim_{k\to 0} \frac{-pk_I m_I[1 + i(2\ln(k_M e)/p)](-k_I a/2)}{2pam_M\{k_I m_I(-k_I a/2)[1 + i(2\ln(k_M a)/p)] - k_M m_M[(2i/k_M ap)]\}}$	
	$= \frac{0}{pm_M^2[(2i/ap)]}$	
	$= 0$	

$$\lim_{b\to 0} p_m^e = \lim_{b\to 0} \frac{pb\,k_I m_I[J_m(k_M e)+iY_m(k_M e)]J_m'(k_I a)}{pam_M\{k_I m_I J_m'(k_I a)[-\,b[J_m(k_M a)+iY_m(k_M a)]+k_M m_M[J_m'(k_M a)+iY_m'(k_M a)]]+b\,k_M m_M J_m(k_I a)[J_m'(k_M a)+iY_m'(k_M a)]\}}$$

Limiting process

$$p_m^e = -\frac{pk_I m_I[J_m(k_M e)+iY_m(k_M e)]J_m'(k_I a)}{pam_M\{k_I m_I J_m'(k_I a)[J_m(k_M a)+iY_m(k_M a)]-\,k_M m_M J_m(k_I a)[J_m'(k_M a)+iY_m'(k_M a)]\}}$$

$$\lim_{k\to 0} p_m^e = \lim_{k\to 0} -\frac{pk_I m_I[J_m(k_M e)+iY_m(k_M e)]J_m'(k_I a)}{pam_M\{k_I m_I J_m'(k_I a)[J_m(k_M a)+iY_m(k_M a)]-\,k_M m_M J_m(k_I a)[J_m'(k_M a)+iY_m'(k_M a)]\}}$$

$$= \lim_{k\to 0} \frac{pk_I m_I}{pam_M\{\dfrac{k_M m_M J_m(k_I a)[J_m'(k_M a)+iY_m'(k_M a)]}{[J_m(k_M e)+iY_m(k_M e)]J_m'(k_I a)} - \dfrac{k_I m_I J_m'(k_M a)+iY_m'(k_M a)]}{[J_m(k_M e)+iY_m'(k_M e)]J_m'(k_I a)}\}}$$

$$= \lim_{k\to 0} \frac{pk_I m_I}{pam_M[\dfrac{k_M m_M J_m(k_I a)Y_m'(k_M a)}{Y_m(k_M e)J_m'(k_I a)} - \dfrac{k_I m_I Y_m(k_M a)}{Y_m(k_M e)}]}$$

$$= \lim_{k\to 0} \frac{pm_I}{pam_M[\dfrac{(k_M/k_I)m_M[(\frac{1}{2}k_I a)^m/m!][m!/2p(\frac{1}{2}k_M a)^{m+1}]}{[-(m-1)!/p(\frac{1}{2}k_M e)^m][(\frac{1}{2}k_I a)^{m-1}/2(m-1)!]} - \dfrac{m_I[-(m-1)!/p(\frac{1}{2}k_M a)^m]}{[-(m-1)!/p(\frac{1}{2}k_M e)^m]}]}$$

Limiting process

$$= \frac{pm_I}{pam_M[-\,m_M(\frac{e}{a})^m - m_I(\frac{e}{a})^m]}$$

$$= \frac{-\,pm_I(\frac{a}{e})^m}{pam_M(m_M+m_I)}$$

$$s_{zr}^{\star} = \frac{m_I}{p(m_I+m_M)}\sum_{m=1}^{\infty}{}' (\frac{a}{e})^m \cos(mq)$$

Case 2

$$s_{zr}^{\star} = \frac{a}{p} s_{zr}^{M} = -\frac{a}{p} m_M [p_0^e + \sum_{m=1}^{\infty} p_m^e \cos(mq)] \text{ for the ideally bonded interface and a concentrated force in the inclusion}$$

$$\lim_{b} p_0^e = \lim_{b} \frac{pb k_M m_I J_0(k_I e)[J_0'(k_M a) + iY_0'(k_M a)]}{2pam_M\{k_I m_I J_0'(k_I a)[- b[J_0(k_M a) + iY_0(k_M a)] + k_M m_M[J_0'(k_M a) + iY_0'(k_M a)]] + bk_M m_M J_0(k_I a)[J_0'(k_M a) + iY_0'(k_M a)]\}}$$

$$= \frac{pk_M m_I J_0(k_I e)[J_0'(k_M a) + iY_0'(k_M a)]}{2pam_M\{- k_I m_I J_0'(k_I a)[J_0(k_M a) + iY_0(k_M a)] + k_M m_M J_0(k_I a)[J_0'(k_M a) + iY_0'(k_M a)]\}}$$

process

$$\lim_{k\to 0} p_0^e = \lim_{k\to 0} \frac{pk_M m_I J_0(k_I e)[J_0'(k_M a) + iY_0'(k_M a)]}{2pam_M\{- k_I m_I J_0'(k_I a)[J_0(k_M a) + iY_0(k_M a)] + k_M m_M J_0(k_I a)[J_0'(k_M a) + iY_0'(k_M a)]\}}$$

$$= \lim_{k\to 0} \frac{pm_I}{2pam_M\{- \dfrac{k_I m_I J_0'(k_I a)[J_0(k_M a) + iY_0(k_M a)]}{k_M J_0(k_I e)[J_0'(k_M a) + iY_0'(k_M a)]} + \dfrac{k_M m_M J_0(k_I a)[J_0'(k_M a) + iY_0'(k_M a)]}{k_M J_0(k_I e)[J_0'(k_M a) + iY_0'(k_M a)]}\}}$$

Limiting

$$= \lim_{k\to 0} \frac{pm_I}{2pam_M[- \dfrac{k_I m_I(- k_I a/2)(2/p)\ln(k_M a)}{k_M(2/pk_M a)} + \dfrac{m_M J_0(k_I a)}{J_0(k_I e)}]}$$

$$= \frac{pm_I}{2pam_M^2}$$

$$\lim_{b\to 0} p_m^e = \lim_{b\to 0} \frac{pbk_M m_I J_m(k_I e)[J_m'(k_M a)+iY_m'(k_M a)]}{pam_M\{k_I m_I J_m'(k_I a)[-\,b[J_m(k_M a)+iY_m(k_M a)]+k_M m_M[J_m'(k_M a)+iY_m'(k_M a)]]+bk_M m_M J_m(k_I a)[J_m'(k_M a)+iY_m'(k_M a)]\}}$$

$$p_m^e = \frac{pk_M m_I J_m(k_I e)[J_m'(k_M a)+iY_m'(k_M a)]}{pam_M\{-\,k_I m_I J_m'(k_I a)[J_m(k_M a)+iY_m(k_M a)]+k_M m_M J_m(k_I a)[J_m'(k_M a)+iY_m'(k_M a)]\}}$$

Limiting process

$$\lim_{k\to 0} p_m^e = \lim_{k\to 0} \frac{pk_M m_I J_m(k_I e)[J_m'(k_M a)+iY_m'(k_M a)]}{pam_M\{-\,k_I m_I J_m'(k_I a)[J_m(k_M a)+iY_m(k_M a)]+k_M m_M J_m(k_I a)[J_m'(k_M a)+iY_m'(k_M a)]\}}$$

$$= \lim_{k\to 0} \frac{pm_I}{pam_M\{\dfrac{-\,k_I m_I J_m'(k_I a)[J_m(k_M a)+iY_m(k_M a)]}{k_M J_m(k_I e)[J_m'(k_M a)+iY_m'(k_M a)]}+\dfrac{k_M m_M J_m(k_I a)[J_m'(k_M a)+iY_m'(k_M a)]}{k_M J_m(k_I e)[J_m'(k_M a)+iY_m'(k_M a)]}\}}$$

$$= \lim_{k\to 0} \frac{pm_I}{pam_M[\dfrac{-\,k_I m_I J_m'(k_I a)Y_m(k_M a)]}{k_M J_m'(k_I e)Y_m'(k_M a)]}+\dfrac{m_M J_m(k_I a)}{J_m(k_I e)}]}$$

Limiting process

$$= \lim_{k\to 0} \frac{pm_I}{-\,(k_I/k_M)m_I[(\frac{1}{2}k_I a)^{m-1}/2(m-1)!][-\,(m-1)!/p(\frac{1}{2}k_M a)^m]}{pam_M[\dfrac{m_M[(\frac{1}{2}k_I a)^m/m!]}{[(\frac{1}{2}k_I e)^m/m!][m!/2p(\frac{1}{2}k_M a)^{m+1}]}+\dfrac{m_M[(\frac{1}{2}k_I a)^m/m!]}{[(\frac{1}{2}k_I e)^m/m!]}]}$$

$$= \frac{pm_I}{pam_M[m_I(\frac{a}{e})^m+m_M(\frac{a}{e})^m]}$$

$$= \frac{pm_I(\frac{e}{a})^m}{pam_M(m_M+m_I)}$$

$$s_{zr}^{\star} = \frac{m_I}{2pm_M}+\frac{m_I}{p(m_I+m_M)}\sum_{m=1}^{\infty}(\frac{a}{e})^m\cos(mq)$$

Appendix C Special cases of $\beta \to \infty$ and $\beta = 0$

Case 1: an ideally bonded case ($\beta \to \infty$)

As the parameter β approaches ∞, the interface condition yields the force equilibrium and displacement continuity. Then, we follow the formulation for the Helmholtz problem in the case 1. For the problem with an inclusion, we can decompose into subsystems of matrix and inclusion after taking free body on the interface as shown in Fig. 1(c). By collocating x on (a^-, ϕ) and (a^+, ϕ) for the matrix and inclusion, respectively, the null-field equations yield Eqs. (17) and (18). Then, the interface conditions of Eq. (5) can be rewritten as

$$u^M = u^I, \quad \text{on the interface} \tag{C1}$$

$$-\mu_M t^M = \mu_I t^I, \quad \text{on the interface} \tag{C2}$$

By assembling the matrices in Eqs. (17), (18), (C1) and (C2), we have

$$\begin{bmatrix} T_{11}^M & -U_{11}^M & 0 & 0 \\ 0 & 0 & T_{11}^I & -U_{11}^I \\ 0 & \mu_M & 0 & \mu_I \\ I & 0 & -I & 0 \end{bmatrix} \begin{bmatrix} u_1^M \\ t_1^M \\ u_1^I \\ t_1^I \end{bmatrix} = \begin{bmatrix} \frac{p}{\mu_M} U(\xi, x) \\ 0 \\ 0 \\ 0 \end{bmatrix} \tag{C3}$$

After rearranging Eq. (C3), we have

$$\begin{bmatrix} T_{11}^M & -U_{11}^M \\ T_{11}^I & \frac{\mu_M}{\mu_I} U_{11}^I \end{bmatrix} \begin{bmatrix} u_1^M \\ t_1^M \end{bmatrix} = \begin{bmatrix} \frac{p}{\mu_M} U(\xi, x) \\ 0 \end{bmatrix} \tag{C4}$$

The unknown coefficients in the algebraic system can be determined as shown below:

$$\begin{aligned} a_0^e = & -pJ_0(k_I a)[J_0(k_M e) + iY_0(k_M e)] \\ & /2\pi a \Big\{ -k_I \mu_I J_0'(k_I a)[J_0(k_M a) + iY_0(k_M a)] \\ & + k_M \mu_M J_0(k_I a)[J_0'(k_M a) + iY_0'(k_M a)] \Big\} \end{aligned} \tag{C5}$$

$$\begin{aligned} p_0^e = & -pk_I \mu_I J_0'(k_I a)[J_0(k_M e) + iY_0(k_M e)] \\ & /2\pi a \mu_M \Big\{ k_I \mu_I J_0'(k_I a)[J_0(k_M a) + iY_0(k_M a)] \\ & - k_M \mu_M J_0(k_I a)[J_0'(k_M a) + iY_0'(k_M a)] \Big\} \end{aligned} \tag{C6}$$

$$\begin{aligned} a_m^e = & -pJ_m(k_I a)[J_m(k_M e) + iY_m(k_M e)] \\ & /\pi a \Big\{ -k_I \mu_I J_m'(k_I a)[J_m(k_M a) + iY_m(k_M a)] \\ & + k_M \mu_M J_m(k_I a)[J_m'(k_M a) + iY_m'(k_M a)] \Big\} \end{aligned} \tag{C7}$$

$$\begin{aligned} p_m^e = & -pk_I \mu_I J_m'(k_I a)[J_m(k_M e) + iY_m(k_M e)] \\ & /\pi a \mu_M \Big\{ k_I \mu_I J_m'(k_I a)[J_m(k_M a) + iY_m(k_M a)] \\ & - k_M \mu_M J_m(k_I a)[J_m'(k_M a) + iY_m'(k_M a)] \Big\} \end{aligned} \tag{C8}$$

where a_0^e, p_0^e, a_m^e and p_m^e, $m = 1, 2, 3, \ldots$ are the Fourier coefficients of boundary densities for the matrix. According to the interface boundary condition of Eqs. (C1) and (C2), we obtain the coefficient of the inclusion as shown below:

$$\begin{Bmatrix} a_0^i \\ p_0^i \end{Bmatrix} = \begin{Bmatrix} a_0^e \\ -\mu_M p_0^e / \mu_I \end{Bmatrix} \tag{C9}$$

$$\begin{Bmatrix} a_m^i \\ p_m^i \end{Bmatrix} = \begin{Bmatrix} a_m^e \\ -\mu_M p_m^e / \mu_I \end{Bmatrix} \tag{C10}$$

where a_0^i, p_0^i, a_m^i and p_m^i are the Fourier coefficients of boundary densities for the inclusion. Then, we can obtain the series-form Green's function for the matrix and the inclusion, respectively, by applying Eq. (9) to have

$$\begin{aligned} G(x, \xi) = & -\frac{\pi a}{2}[a_0^e k_M J_0'(k_M a) + p_0^e J_0(k_M a)] \\ & [Y_0(k_M \rho) - iJ_0(k_M \rho)] \\ & - \frac{\pi a}{2} \sum_{m=1}^{\infty} [a_m^e k_M J_m'(k_M a) + p_m^e J_m(k_M a)] \\ & [Y_m(k_M \rho) - iJ_m(k_M \rho)] \cos(m\phi) \\ & - \frac{p}{4\mu_M}[Y_0(k_M r) - iJ_0(k_M r)], \quad a \le \rho < \infty \end{aligned} \tag{C11}$$

$$G(x,\xi)=\frac{\pi a}{2}J_0(k_I\rho)\left\{a_0^i k_I[Y_0'(k_I a)-iJ_0'(k_I a)]\right.$$
$$\left.-p_0^i[Y_0(k_I a)-iJ_0(k_I a)]\right\}$$
$$\frac{\pi a}{2}J_m(k_I\rho)\left\{a_m^i k_I[Y_m'(k_I a)-iJ_m'(k_I a)]\right.$$
$$\left.-p_m^i[Y_m(k_I a)-iJ_m(k_I a)]\right\},\quad 0<\rho<a \tag{C12}$$

The absolute amplitude of potential $|u|$ for the ideally bonded case and for the parameter $(\beta=10^{32})$ are shown in Figs. 12 and 13. Good agreement is made.

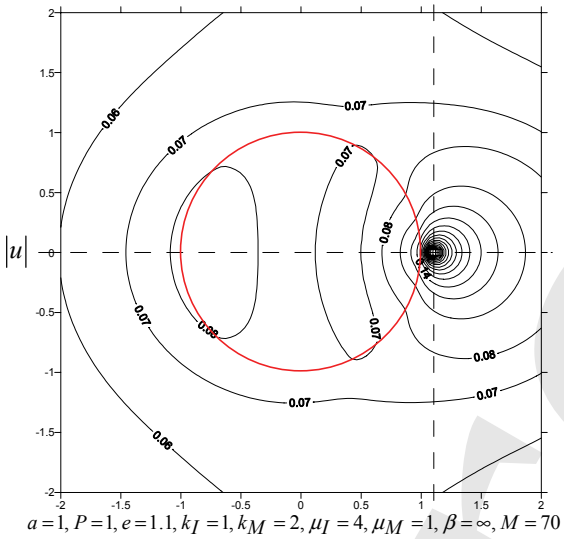

Figure 12: The absolute amplitude of displacement for an ideally bonded case

Case 2: a cavity case $(\beta=0)$

As the parameter β is zero as shown in Fig. 14, the circular inclusion is fully debonded from the matrix. Similarly as shown in the case 1, we can obtain the unknown coefficients as shown below:

$$\begin{bmatrix}a_0^e\\ a_m^e\end{bmatrix}=\begin{bmatrix}\frac{-p}{2k_M\pi a\mu_M}\frac{Y_0(k_M e)-iJ_0(k_M e)}{Y_0'(k_M a)-iJ_0'(k_M a)}\\ \frac{-p}{k_M\pi a\mu_M}\frac{Y_m(k_M e)-iJ_m(k_M e)}{Y_m'(k_M a)-iJ_m'(k_M a)}\end{bmatrix} \tag{C13}$$

where a_0^e and a_m^e, $m=1,2,3,\ldots$ are the Fourier coefficients of boundary densities for the matrix. Then, we can obtain the series-form Green's function for the matrix by applying Eq. (9) to have

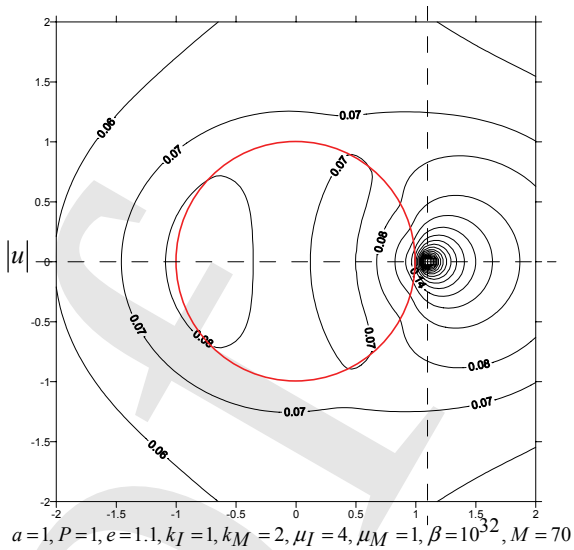

Figure 13: The absolute amplitude of displacement for $\beta=10^{32}$

$$G(x,\xi)=$$
$$-\frac{\pi a}{2}a_0^e k_M J_0'(k_M a)[Y_0(k_M\rho)-iJ_0(k_M\rho)]$$
$$-\frac{\pi a}{2}\sum_{m=1}^{\infty}a_m^e k_M J_m'(k_M a)$$
$$[Y_m(k_M\rho)-iJ_m(k_M\rho)]\cos(m\phi)$$
$$-\frac{p}{4\mu_M}[Y_0(k_M r)-iJ_0(k_M r)],\quad a\le\rho<\infty \tag{C14}$$

The absolute amplitude of potential $|u|$ for the cavity case and for the parameter$(\beta=10^{-32})$ are shown in Figs. 15 and 16. Good agreement is also made.

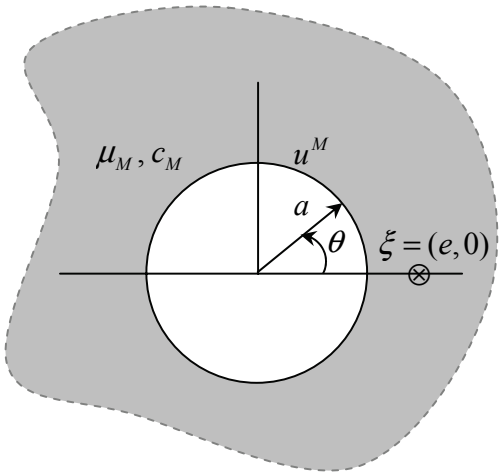

Figure 14: A matrix with a debonded inclusion

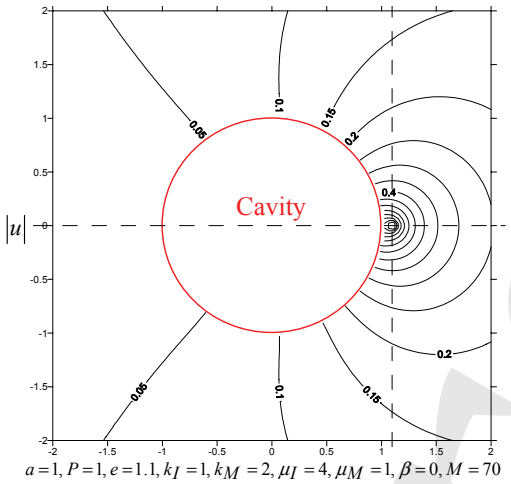

Figure 15: The absolute amplitude of displacement for the cavity

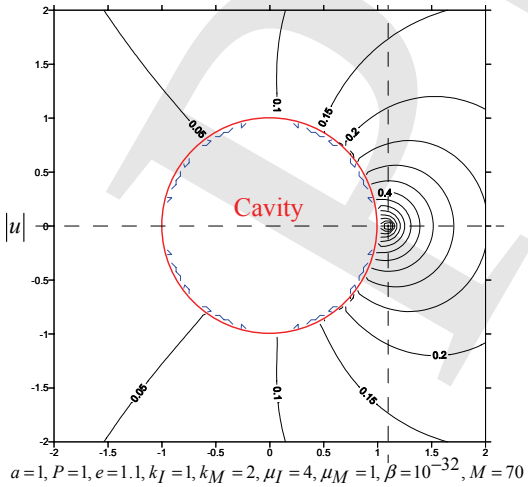

Figure 16: The absolute amplitude of displacement for $\beta = 10^{-32}$